

**Enterobacteriaceae host adaptation driven by intestinal ethanolamine**

Carol Rowley

Oak Park, Illinois

B.S. University of Notre Dame, 2013

A Dissertation presented to the Graduate Faculty  
of the University of Virginia in Candidacy for the Degree of  
Doctor of Philosophy

Department of Microbiology, Immunology, and Cancer Biology

University of Virginia

April 2020

## TABLE OF CONTENTS

<b>List of abbreviations</b> .....	i
<b>Abstract</b> .....	iii
<b>Acknowledgements</b> .....	v
<b>Chapter 1: Introduction to ethanolamine utilization in Enterobacteriaceae</b> .....	1
Bacterial intestinal adaptation.....	2
Enterobacteriaceae.....	5
EA utilization.....	9
Enteric pathogen transmission.....	13
Figures.....	15
<b>Chapter 2: Human commensal <i>Escherichia coli</i> grow, alter gene expression, and outcompete enterohemorrhagic <i>E. coli</i> O157:H7 using ethanolamine</b> .....	17
Abstract.....	18
Introduction.....	19
Results.....	19
Discussion and Future Directions.....	22
Materials and Methods.....	27
Figures.....	30
<b>Chapter 3: <i>Citrobacter rodentium</i> ethanolamine utilization contributes to intestinal virulence, colonization, and transmission</b> .....	37
Abstract.....	38
Introduction.....	39
Results.....	40
Discussion and Future Directions.....	48
Materials and Methods.....	55
Figures.....	63
<b>Chapter 4: Summary and implications to the field</b> .....	77
Summary.....	78
Implications to the Field.....	79
Figure.....	82
<b>Appendix</b>	
Table 1. Bacterial strains used in Chapter 2.....	83
Table 2. Oligonucleotides used in Chapter 2.....	84
Table 3. Bacterial strains used in Chapter 3.....	85
Table 4. Oligonucleotides used in Chapter 3.....	86
<b>References</b> .....	88

## LIST OF ABBREVIATIONS

**AdoCbl:** adenosylcobalamin (vitamin B<sub>12</sub>)

**AE lesion:** attaching and effacing lesion

**CFU:** colony forming units

**ChIP-qPCR:** chromatin immunoprecipitation and quantitative polymerase chain reaction

**ChIP-seq:** chromatin immunoprecipitation and sequencing

**DMEM:** Dulbecco's modified Eagle's medium

**EA:** ethanolamine

**EHEC:** enterohemorrhagic *Escherichia coli* O157:H7

**EMSA:** electrophoretic mobility shift assay

***eut* operon:** EA utilization operon

**GI:** gastrointestinal

**HS:** *Escherichia coli* HS

**HUS:** hemolytic-uremic syndrome

**IQR:** interquartile range

**IVIS:** *in vivo* imaging system

**LB:** Luria broth

**LEE:** locus of enterocyte effacement

**LOD:** limit of detection

**Nissle:** *Escherichia coli* Nissle

**RNA-seq:** RNA-sequencing

**RT-qPCR:** quantitative reverse transcription polymerase chain reaction

**SD:** standard deviation

**SNPs:** single nucleotide polymorphisms

**Stx:** Shiga toxin

**T3SS:** type III secretion system

**Tir:** translocated intimin receptor

## ABSTRACT

Elucidating the role of metabolites and signaling molecules used by the microbiota and pathogens is critical to develop strategies to support intestinal homeostasis and to prevent pathogenic infection. Utilization of the nutrient ethanolamine (EA) by commensal bacteria and enteric pathogens remains incompletely understood and has important implications for human health. The dogma of the EA utilization field had been that pathogens metabolize EA as a noncompetitive metabolite, based on one study that examined expression of EA utilization (*eut*) genes by bovine commensal *Escherichia coli*. The view of EA as a metabolite that is specifically used by pathogens as a way to overcome commensal nutritional competition has broad implications for our understanding of EA use in the intestinal tract. However, limitations of the aforementioned study led us to re-examine EA utilization by human commensal *E. coli*. We hypothesized that commensal *E. coli*, which encode conserved *eut* loci with pathogenic Enterobacteriaceae, would respond to EA to promote *eut* gene expression and growth using EA. In Chapter 2, we demonstrate that EA supports human commensal *E. coli* gene expression and growth, resulting in outgrowth compared to the enteric pathogen enterohemorrhagic *E. coli* O157:H7 (EHEC) in co-culture. Additionally, commensal *E. coli* sense EA to alter fimbrial gene expression, which may impact host colonization. Therefore, our data challenge the dogma that pathogens preferentially utilize EA and demonstrate that commensal *E. coli* sense EA to alter gene expression and promote metabolism. Unlike commensal *E. coli*, EHEC is a foodborne pathogen with significant morbidity and mortality, and an extremely low infectious dose is sufficient to cause disease. Without therapeutic options to treat EHEC infection, better understanding of EHEC pathogenesis is critical. Before this work, the role of the *eut* operon transcriptional regulator EutR in EHEC intestinal pathogenesis remained to be elucidated. In Chapter 3, we use the murine model of EHEC infection,

*Citrobacter rodentium*, to show that EutR impacts virulence and colonization in the intestinal tract. Additionally, a critically important but understudied area of enteric pathogenesis is the ability to transmit to naïve hosts. We demonstrate that EutR-dependent gene expression promotes effective transmission to naïve hosts to contribute to pathogen propagation in a host population. Together, these studies expand our understanding of intestinal metabolism and signaling in host-pathogen-microbiota interactions.

## ACKNOWLEDGEMENTS

I would first like to thank my mentor, Melissa Kendall, for continual guidance and encouragement throughout my graduate career. Melissa has been a supportive mentor and has challenged me to grow towards becoming the best scientist I can be. Having been a runner for many years, I also appreciated that Melissa understood my need to destress through running and even encouraged me to run on tough days. The Kendall lab members have made both an intellectually stimulating and fun environment to work in, especially those members with whom most of my graduate career overlapped: Beth, Brooke, and John. I have enjoyed spending my workdays surrounded by interesting people with a love of science and compatible senses of humor. My experimental plans and interpretation of data have been impacted greatly by informal lab chats in our office space over the years.

I would also like to thank the members of my thesis committee for their regular support and ideas during my training: Drs. Hervé Agaisse, Jim Casanova, Melanie Rutkowski, and Tim Bender. My committee was readily available to talk through any issues I needed guidance on and shared their time to ensure that my science was performed and presented in a rigorous manner.

I also want to thank the amazing friends I have from home in Chicago, from college, and those I have made in Charlottesville. Through the graduate school, medical school, and the running communities in Charlottesville, I have made some of the most important friendships of my life, and they have been so important in keeping me sane throughout this process.

Finally, I'd like to thank my family. My parents, Drs. Anne and Stephen Rowley, have been nothing but supportive throughout my many schooling years, encouraging me to follow my interests wherever they lead. I'd especially like to thank my mother, who was my first scientist role model and has inspired me to follow in her footsteps to pursue my

research interests in the field of infectious diseases. My siblings, Colleen and Mike, and siblings-in-law, Bill and Abby, have also been a wonderful source of support. They have additionally provided maybe the greatest distraction and source of laughter through my niece Ellie and nephews Sam and William.

**Chapter 1: Introduction to ethanolamine utilization in Enterobacteriaceae**

Part of this chapter has been adapted from “To B12 or not to B12: Five questions on the role of cobalamin in host-microbial interactions.”

Carol A. Rowley and Melissa M. Kendall. 2019. PLoS Pathog. 15(1): e1007479.

Nonpathogenic and pathogenic bacteria utilize metabolites to grow and alter gene expression to adapt to the intestinal niche (1). The mammalian intestinal tract provides a plentiful source of nutrients for microbes. Thus, commensal bacteria that make up the resident microbiota have evolved to metabolize these nutrients to promote colonization of the intestinal tract, often acting in symbiosis with the host by promoting digestion and preventing pathogenic infection (2, 3). To effectively compete with the microbiota, pathogens have evolved additional strategies to acquire nutrients that promote growth in this environment and transmission within a host population. EA is metabolite that is released into the intestinal tract through cell membrane turnover. EA has been thought to promote the growth and gene expression of pathogens but not of nonpathogenic members of the resident microbiota. In this dissertation, we demonstrate that commensal *E. coli* use EA as a metabolite and as a signal to alter gene expression. The transcriptional regulator EutR, which controls the expression of genes that promote EA metabolism in Enterobacteriaceae, also regulates pathogen virulence gene expression. Using the *C. rodentium* mouse model of EHEC infection, we demonstrate that EutR-dependent gene regulation promotes virulence, colonization, and transmission to naïve hosts. In this introduction, we discuss bacterial intestinal adaptation, Enterobacteriaceae, EA utilization, and enteric pathogen transmission.

## **Bacterial intestinal adaptation**

### The resident microbiota and colonization resistance to pathogens

The resident microbiota has evolved to occupy the human intestinal niche and typically grows in the lumen or outer mucus layer (Fig. 1-1A inset). The resident microbiota is composed of bacteria that benefit the host in numerous ways. The microbiota ferments complex carbohydrates obtained from the diet and releases short-chain fatty acids as a

byproduct, which in turn support epithelial cell metabolism and host cell differentiation (4-6). Additionally, the microbiota modifies bile acids, which are toxic to the bacteria, altering the bile acid structures into forms that are critical for host cell signaling and modulate disease processes (7). About 160 unique bacterial species are found in a healthy human colon (8), and each needs to acquire sufficient sources of carbon, nitrogen, and vitamins to survive. Therefore, members of the resident microbiota use a variety of strategies to acquire nutrients without harming their host. The host diet, the mucus layer, and the turnover of host epithelial cells and bacterial cells provide valuable nutrient sources for the microbiota (5, 6). Additionally, most members of the microbiota encode transport systems (such as cobalamin / vitamin B<sub>12</sub> uptake proteins (9)) to obtain cofactors from the host environment that aid in metabolism and other enzymatic processes. This symbiotic relationship between the host and the microbiota promotes microbiota occupation of this niche to maintain a healthy intestinal environment and prevent pathogen infection.

The microbiota provides colonization resistance against pathogenic infection by competing with pathogens for available metabolites (3). To effectively colonize the intestinal tract, pathogens have developed mechanisms to overcome this challenge and acquire sufficient nutrients. These strategies involve metabolizing different nutrient sources from the microbiota, occupying distinct intestinal niches from the microbiota, and/or disrupting the host environment to release additional nutrients (1). While members of the microbiota are commonly located in the outer mucus layer of the colon, some pathogens can reach the host epithelial layer to take advantage of unique nutritional opportunities. For example, pathogen-induced inflammation at the epithelial layer promotes generation of an alternative electron acceptor, which allows *Salmonella* Typhimurium to gain a growth benefit through metabolism of intestinal EA (10). Using

these strategies, pathogens overcome colonization resistance to adapt to the intestinal tract.

#### Metabolites as effector ligands that promote niche adaptation

The microbiota and pathogens utilize endogenous metabolites to sense the host environment, which promotes gene expression that allows for adaptation. Some metabolites act as effector ligands that alter the expression of genes involved in catabolism or biosynthesis of that metabolite. Through this mechanism, bacteria sense the surrounding environment to enhance expression of metabolic proteins and/or repress expression of proteins involved in biosynthesis when the metabolite is available (11). For example, in *E. coli*, the amino acid arginine binds to the ArgR transcription factor, which regulates hundreds of genes involved in arginine metabolism and biosynthesis (12). Pathogens have developed additional strategies to utilize host-derived molecules to regulate virulence gene expression, resulting in harm to the host (6). For example, the enteric pathogen EHEC uses the abundant mucin-derived metabolite fucose as an effector ligand that alters signal transduction through the two-component regulatory system FusKR to affect virulence and colonization (13). In a different example, microbiota-derived indole decreases activity of the EHEC two-component regulatory system CpxA-CpxR, which leads to inhibition of virulence gene expression (14). Because indole concentrations are higher in the luminal content than at the epithelial layer, EHEC uses indole to sense the environment and upregulate virulence gene expression upon entering the host niche at the colonic epithelium. Through sensing the intestinal environment, the microbiota and pathogens finely coordinate gene expression.

## Enterobacteriaceae

Enterobacteriaceae are a family of Gram-negative facultative anaerobes that include nonpathogenic and pathogenic species, which colonize a wide variety of environmental and host-associated niches (15). The Enterobacteriaceae include commensal *E. coli* and the clinically important pathogens EHEC, enteropathogenic *E. coli* (EPEC), *Salmonella enterica* serovar Typhi, *Klebsiella pneumoniae*, *Shigella flexneri* and *dysenteriae*, *Yersinia pestis*, and *Enterobacter faecalis* and *cloacae*, for example. Pathogenic Enterobacteriaceae infect the bloodstream, lungs, lymphatic system, skin, and intestinal tract (15). *E. coli* includes a diverse group of intestinal commensal strains and pathogenic strains that infect distinct host niches. Strains of extra-intestinal pathogenic *E. coli* (ExPEC) can cause urinary tract infections, meningitis, and bacteremia (16). Pathogenic *E. coli* that cause intestinal disease and severe diarrhea include EHEC and EPEC.

### Commensal *E. coli*

Commensal *E. coli* grow in the lumen and outer mucus layer of the human colon and compose about 0.1% of the resident microbiota (17). Commensal *E. coli* form a symbiotic relationship with the human host, aiding in colonization resistance against pathogenic infection through nutritional competition (2). Various strains of species-specific commensal *E. coli* can be found in the intestinal tract, each with slight genomic variations. On average, five unique *E. coli* strains are detected in a human's stool (18). *E. coli* HS is one nonpathogenic strain of human commensal *E. coli* that was isolated from a healthy individual and is commonly used in laboratory studies (19-21). *E. coli* Nissle is another human *E. coli* strain that was isolated during a *Shigella* outbreak from a German soldier during World War I who showed no signs of disease (22, 23). *E. coli* Nissle has unique

anti-pathogenic properties and is the active ingredient in the probiotic “Mutaflor” (24). Overall, commensal *E. coli* colonize the human intestinal tract without harming the host and provide additional host benefits.

## EHEC

EHEC is a pathogenic serotype of *E. coli* that causes an estimated 73,000 cases in the US annually (25). Ingestion of as low as 50-100 colony forming units (CFU) is sufficient to cause infection (26), making EHEC a major public health concern. EHEC colonizes cattle asymptotically (27), and food products contaminated with bovine feces are common sources of infection. These include undercooked hamburger meat and romaine lettuce. A significant proportion of infections, especially in young children, also occur via direct person-to-person contact (28, 29). Following an average incubation period of 3-4 days, patients present with diarrhea that progresses to hemorrhagic colitis, causing bloody diarrhea with severe abdominal cramping (30). Hemorrhagic colitis is caused by the virulence factor Shiga toxin (Stx), which is encoded by EHEC. After one week of diarrhea, the GI symptoms generally resolve. However, as intestinal symptoms improve, Stx circulates through the host bloodstream and can cause hemolytic-uremic syndrome (HUS), the most severe complication of EHEC infection. HUS is characterized by the triad of hemolytic anemia, thrombocytopenia, and acute kidney injury and occurs in 5-15% of cases (31), especially in the young and elderly. Antibiotic therapy increases the production of Stx and the risk of HUS (32); therefore, treatment of EHEC infection is limited to supportive care.

Ingested EHEC colonizes the colon, where EHEC expresses adhesins that are thought to promote early attachment to the epithelium (33, 34). On host epithelial cells, EHEC expresses a type III secretion system (T3SS). The T3SS is a syringe-like structure

that allows injection of bacterial effectors into the host cytosol that modulate host processes (35). EHEC translocates its own receptor, translocated intimin receptor (Tir), through the T3SS, which localizes to the host membrane and binds to the extracellular EHEC receptor, intimin (36). Other effectors cause host cytoskeletal rearrangement and formation of a pedestal-like structure called an attaching and effacing (AE) lesion, to which EHEC attaches extracellularly (Fig. 1-1A inset) (36). The T3SS structural components and most secreted effectors are encoded by genes carried in the locus of enterocyte effacement (LEE), a 35-kb pathogenicity island critical for EHEC virulence that is organized into five operons (37). The LEE-encoded-regulator (Ler) is encoded as the first gene of the *LEE1* operon and regulates transcriptional expression of the LEE (38). Unsurprising given the central role of the LEE in EHEC virulence, Ler expression is highly regulated (39). In addition to LEE-encoded effectors, several non-LEE-encoded effectors encoded at distinct genomic locations are also secreted through the T3SS (40). In total, 49 putative T3SS effectors have been identified in EHEC and 40 have been experimentally validated (41, 42). In addition to promoting AE lesion formation, these effectors have roles in host immune modulation during infection (43). Following LEE-dependent colonization, EHEC expresses Stx, which inhibits protein synthesis and causes symptoms of hemorrhagic colitis and HUS, as previously discussed (31).

#### Animal models of EHEC infection

Animals models of EHEC pathogenesis have been developed in pigs, rabbits, and monkeys (44), but limited studies have been performed using these models due to their cost and limited genetic tractability. In mice, EHEC colonizes the colon with continuous streptomycin treatment, and this model is useful to investigate EHEC nutritional competition (45, 46). However, EHEC infection of mice does not replicate pathogenesis,

including AE lesion formation. Therefore, a natural mouse AE pathogen, *C. rodentium*, which causes colitis in mice, is commonly used to model EHEC pathogenesis.

### *Citrobacter rodentium*

The mouse-specific Enterobacteriaceae pathogen *C. rodentium* shares 83% and 85% LEE protein sequence homology with EHEC (Fig. 1-1B) (47-52) and the closely related human AE pathogen EPEC, respectively (53). The LEE was likely acquired through plasmid-based horizontal gene transfer independently from a common source in EHEC / EPEC and *C. rodentium* (47). Therefore, *C. rodentium* can be used to model LEE-dependent pathogenesis in mice. *C. rodentium* causes an infection referred to as “transmissible murine colonic hyperplasia,” first described during outbreaks of colitis in laboratory mice (54, 55). Following inoculation of C57BL/6 mice with *C. rodentium* via oral gavage, *C. rodentium* transiently colonizes the cecum by three days post infection (56) and upregulates LEE expression to establish a primary colonic niche by five days post infection (56, 57). In the distal colon, *C. rodentium* expresses the T3SS and secretes effectors, which promote AE lesion formation. During intestinal colonization, *C. rodentium* is shed in the stool and causes mildly loose stools. Mice practice coprophagy to acquire necessary nutrients from their diet (58); therefore, *C. rodentium* shed in stool is effectively transmitted via the fecal-oral route when mice are co-housed. Following host passage, *C. rodentium* acquires a hypervirulent phenotype, requiring 1000-fold fewer bacteria to infect a naïve mouse and localizing to colonic tissue by three days post infection (59, 60). C57BL/6 mice are able to clear *C. rodentium* infection after 2-3 weeks through adaptive immune responses including the production of CD4+ T-cells and B-cells (51).

## EA utilization

### Conserved EA metabolism genes

EA, a component of the integral cell membrane phospholipid phosphatidylethanolamine, is released through cell membrane turnover (61, 62); therefore, EA is a ubiquitous molecule in environments associated with living organisms. Diverse bacteria have evolved to encode genes that promote EA metabolism as a source of carbon, nitrogen, and/or energy (63).

Many bacteria encode conserved genes to metabolize EA, including the well-studied *eut* genes, though non-*eut* mechanisms of EA metabolism have also been reported (64, 65). The most widely conserved *eut* genes encode the EA ammonia lyase, EutBC, which breaks down EA for use as a nitrogen source, releasing ammonia and acetaldehyde. EutBC requires cobalamin (vitamin B<sub>12</sub>) for activity in the form of adenosylcobalamin (AdoCbl) (66, 67). Using genome alignments, conserved *eutBC* genes have been identified in nearly 100 sequenced bacteria. These bacteria include Gram-positive and Gram-negative members, aerobes, facultative anaerobes, and anaerobes, and microbes occupying environmental niches, including soil and the deep ocean, and host niches, including the lung and the intestinal tract (63). These data suggest that EA metabolism is an important mechanism of bacterial nutrient acquisition under a variety of environmental conditions.

While the *eutBC* genes are conserved among bacterial genomes, additional genes that contribute to EA metabolism are encoded only by certain bacterial groups. *Actinobacteria* and some *Proteobacteria*, which include soil-dwelling bacteria that fix nitrogen in addition to important pathogens such as *Mycobacterium tuberculosis* and *M. leprae*, only encode *eutBC* and the EA transporter *eat*. *Eat* promotes the movement of protonated EA across bacterial cell membrane(s) under acidic conditions (63, 68). In

another example, the environmental extremophile *Symbiobacterium thermophilum* and insect pathogen *Photobacterium luminescens* encode only *eutBC* and *eutA*, the “reactivating factor” of EutBC. AdoCbl undergoes irreversible Co-C bond cleavage during EA catabolism, and each round of catalysis requires a new or re-adenosylated cobalamin molecule. EutA removes the unusable cobalamin from the enzyme to allow a new AdoCbl molecule to reactivate EutBC (69). *eutA* is also encoded by the “long *eut* operons” discussed in the following section. Overall, Eat and EutA increase the efficiency of EA metabolism in certain bacteria.

Some bacterial families, including Enterobacteriaceae and Firmicutes, encode a long operon with additional genes to metabolize EA as a nitrogen, carbon, and/or energy source. Enterobacteriaceae encode a 17-gene *eut* operon (Fig. 1-2), while Firmicutes encode a 16-to-17-gene operon (68). Proteins encoded by *eutS*, *eutM*, *eutK*, *eutL*, and *eutN* form the structural components of a microcompartment (70), which increases the local concentrations of enzymes required for EA catabolism (71). Because EutBC activity requires AdoCbl, the adenosyltransferase EutT transfers the adenosine group from ATP to other derivatives of cobalamin to generate AdoCbl (72). Enterobacteriaceae and Firmicutes also encode *eutH*, which forms a transporter protein similar to Eat that facilitates the movement of protonated EA into the cell under acidic conditions (73, 74). EutBC breaks down EA into ammonia, which is readily consumed as a nitrogen source, and the toxic intermediate acetaldehyde. The microcompartment prevents acetaldehyde from entering the cytosol and causing cellular harm (75), and acetaldehyde is further broken down within the microcompartment. EutG converts acetaldehyde into ethanol, which leaves the cell as a harmless byproduct (74), and EutE converts acetaldehyde into acetyl-CoA (67, 76). Acetyl-CoA enters metabolic pathways including the TCA cycle, which is coupled with oxidative phosphorylation to generate ATP. Alternatively, acetyl-

CoA is phosphorylated by EutD and can undergo substrate level phosphorylation, during which acetate kinases EutP and EutQ promote transfer of the phosphate group bound to acetyl-CoA to ADP, generating ATP (77, 78). Overall, the genes encoded by long *eut* operons provide bacteria with strategies to efficiently break down EA for nutritional consumption.

### *eut* operon regulation

While *eut* metabolic proteins encoded by Enterobacteriaceae and Firmicutes are highly conserved, regulation of these *eut* operons is distinct. In Enterobacteriaceae, EutR is the last gene encoded by the *eut* operon and is the transcriptional regulator of *eut* gene expression (79). EutR is a member of the AraC family of bacterial transcription factors, containing a conserved DNA-binding C-terminal domain and a variable ligand-binding N-terminal domain (80). EutR is expressed at low levels from the P2 constitutive promoter (the “*eutR* promoter”) (79) and directly binds to the P1 promoter upstream of the first *eut* gene, *eutS* (the “*eutS* promoter”) (81) (Fig. 1-2). EA is the effector ligand that binds EutR and, in the presence of AdoCbl, promotes expression of the *eut* operon (81), including readthrough of the *eutR* promoter to enhance EutR expression (79).

In the Firmicutes, EA is the effector ligand that initiates phosphorylation of the sensor kinase EutW. This phosphate is then transferred to the noncanonical response regulator EutV (noncanonical because EutV functions post-transcription initiation by binding RNA and preventing formation of transcription-termination structures as opposed to binding DNA). In the absence of AdoCbl, the *eut*-encoded small RNA (sRNA) EutX/Rli55 sequesters EutV, thereby inhibiting EutV antitermination activity. The sRNA contains an AdoCbl-binding domain. AdoCbl binding causes a structural change in EutX/Rli55 that results in transcription termination and production of a truncated sRNA

that cannot sequester EutV (82, 83). Using unique regulatory mechanisms, Enterobacteriaceae and Firmicutes evolved to use the effector ligand EA and AdoCbl to promote *eut* expression.

#### EA metabolism by intestinal bacteria

Both members of the microbiota and pathogens encode *eut* genes and can use EA to grow, but EA is generally thought to be a noncompetitive metabolite associated with pathogenesis that is poorly metabolized by commensals (63, 84). EA metabolism influences pathogen growth and/or virulence in the intestinal tract (*Salmonella* Typhimurium, *Clostridium difficile*, and *Enterococcus faecalis*), at sites of extraintestinal dissemination (*Salmonella* Typhimurium and *Listeria monocytogenes*), and in the urinary tract (uropathogenic *Escherichia coli*) (81, 82, 85-91). Additionally, the pathogens EHEC and *Pseudomonas aeruginosa* grow using EA *in vitro* (84, 92). Therefore, EA is exploited by pathogens for growth. However, use of EA by members of the microbiota remains less well understood; this topic will be further discussed in Chapter 2. Overall, these data demonstrate that EA metabolism plays an important role in pathogen growth and colonization.

#### The role of EA in metabolism-independent gene expression

EA has additional effects on non-metabolic gene expression in Enterobacteriaceae. In *Salmonella enterica* serovar Typhimurium, EutR directly regulates expression of virulence regulator SsrB and enhances intestinal colonization during colitis through EA metabolism and through metabolism-independent mechanisms (86, 87). Additionally, EutR-dependent virulence enhances *S. Typhimurium* survival in the intramacrophage environment (86), suggesting a role for EutR in adaptation to intracellular

host niches in addition to the intestinal tract. In EHEC, EA promotes the expression of fimbriae through EutR-dependent and EutR-independent mechanisms and contributes to epithelial cell adhesion (91). Furthermore, EutR binds directly to the Ler promoter and, when EA and AdoCbl are present, promotes LEE gene expression and AE lesion formation (81). Therefore, EA supports virulence gene expression that contributes to Enterobacteriaceae colonization.

### **Enteric pathogen transmission**

Pathogens that infect the gastrointestinal tract are transmitted to a human host from an environmental reservoir or from an infected person via the fecal-oral route. Common environmental reservoirs include the GI tract of animals and bodies of water (93). Pathogens can infect human hosts through direct contact with an environmental reservoir or, more commonly, through ingestion of contaminated food products or water. Contaminated food commonly includes meat, eggs, and produce. Common foodborne pathogens include EHEC, *Campylobacter jejuni*, and *Salmonella enterica* serovars Typhi and Typhimurium, though these pathogens can also be transmitted through contaminated water (94). *Vibrio cholerae* is primarily spread via a waterborne route, as the bacteria replicate in an environmental niche in brackish water (95).

Enteric pathogens that are transmitted via foodborne or waterborne routes can also be transmitted via person-to-person transmission. Direct person-to-person transmission results from inadequate sanitation and/or poor hygiene practices, which leads to high rates of pathogenic infection in developing nations (96). While direct person-to-person spread is generally of less concern in developed nations, daycare centers remain a major source of direct person-to-person transmission (96). Additionally, enteric infections among non-human mammals are generally spread via direct animal-to-animal

transmission, especially in animals that practice coprophagy, or eating of feces. For example, the murine pathogen *C. rodentium* is effectively transmitted among mice through cohousing (51). Through effective transmission to new hosts, intestinal pathogens can survive in a host population and spread.

## Figures

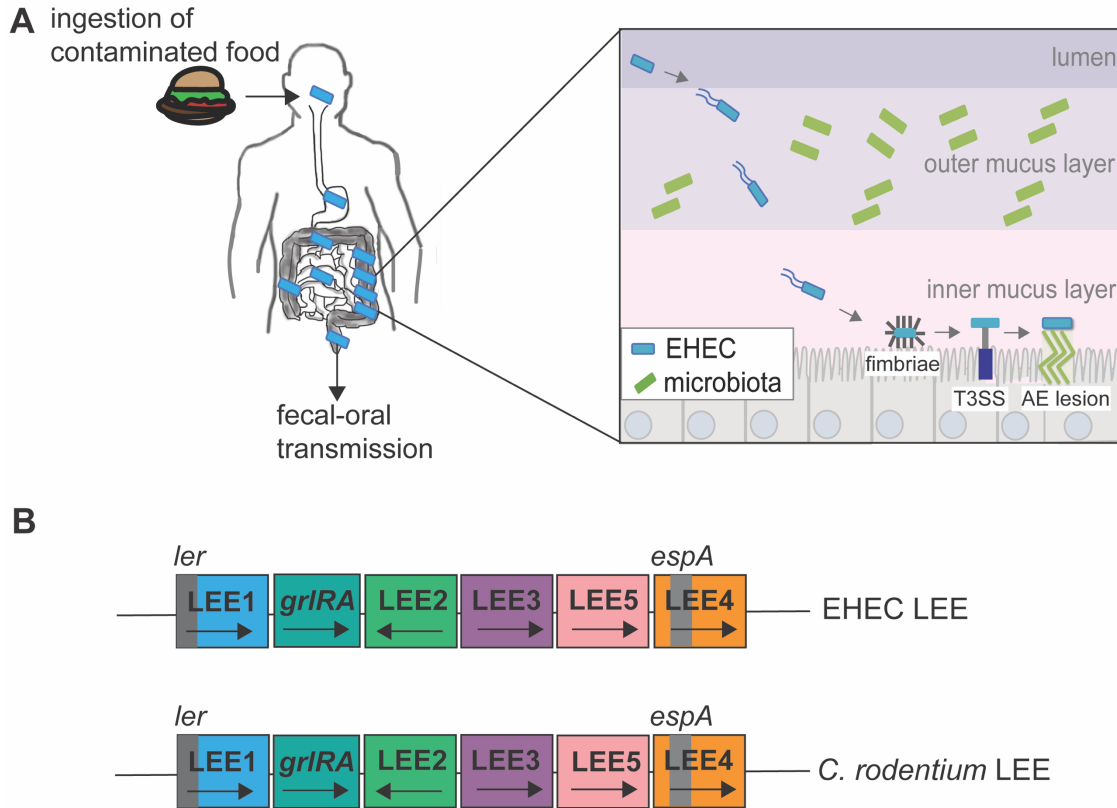


**Fig. 1-1. EHEC intestinal adaptation using the locus of enterocyte effacement (LEE).**

(A) A host ingests a hamburger contaminated with EHEC, which moves through the intestinal tract and colonizes the distal colon. In the inset, EHEC expresses flagella to move through the mucus layers to reach the colonic epithelium. At the epithelial layer, EHEC expresses fimbriae to promote early attachment and then expresses a T3SS, with effectors leading to host cytoskeletal rearrangement and AE lesion formation. During host colonization, EHEC is shed in stool and transmitted via the fecal-oral route. (B) Schematic of the LEE in EHEC and *C. rodentium*.

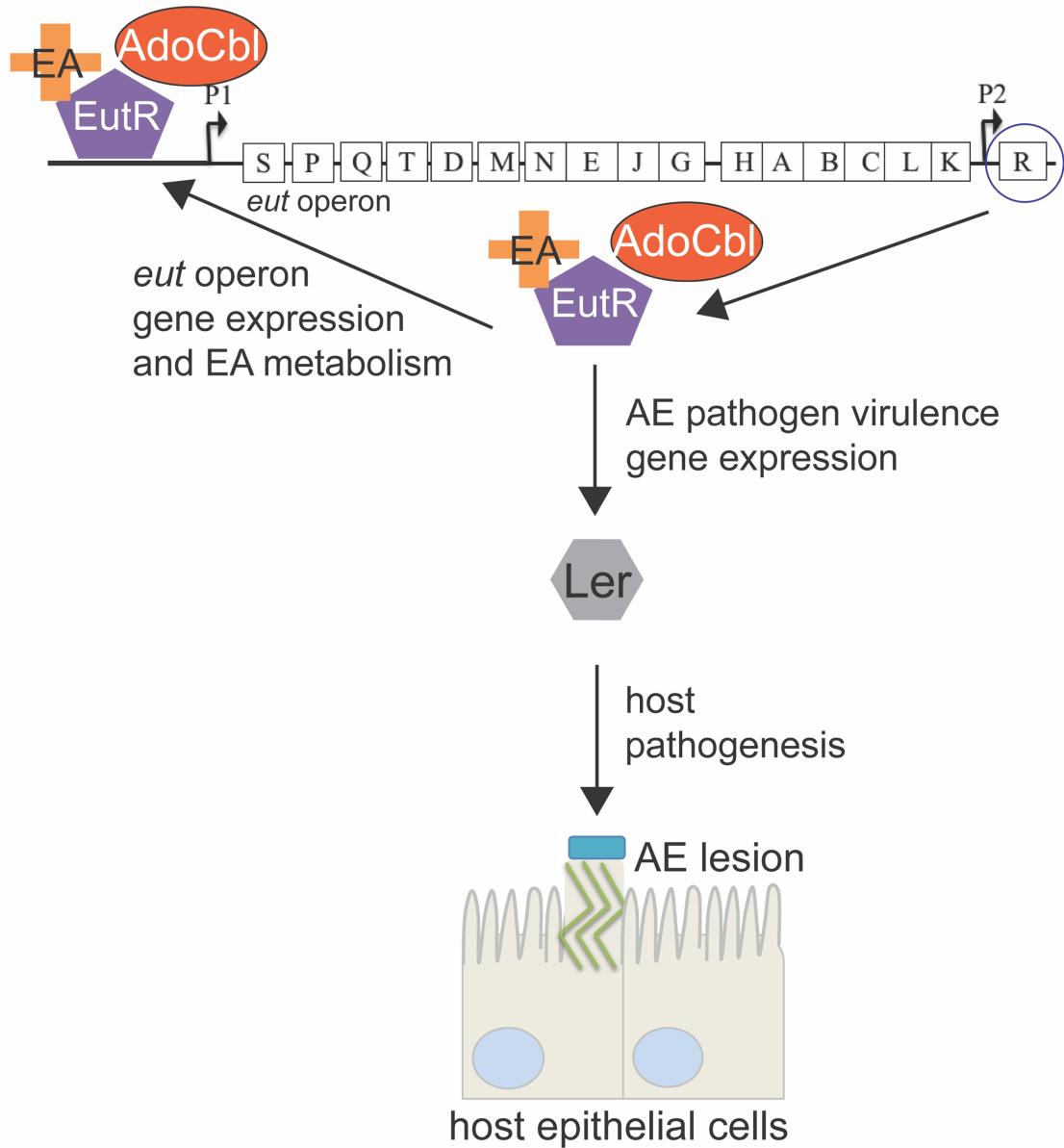


**Fig. 1-2. Ethanolamine utilization in Enterobacteriaceae.**

Schematic of the *eut* operon in Enterobacteriaceae regulated by EutR. EutR with EA and AdoCbl promotes *eut* operon expression and EA metabolism in commensal and pathogenic Enterobacteriaceae. In AE pathogens, EutR also regulates *ler* expression and promotes AE lesion formation.

**Chapter 2: Human commensal *Escherichia coli* grow, alter gene expression, and outcompete enterohemorrhagic *E. coli* O157:H7 using ethanolamine**

Part of this chapter has been adapted from “Ethanolamine Influences Human Commensal *Escherichia coli* Growth, Gene Expression, and Competition with Enterohemorrhagic *E. coli* O157:H7.”

Carol A. Rowley, Christopher J. Anderson, and Melissa M. Kendall. 2018. *mBio*. 9:e01429-18.

## Abstract

A core principle of bacterial pathogenesis is that pathogens preferentially utilize metabolites that commensal bacteria do not in order to sidestep nutritional competition. The metabolite EA is well recognized to play a central role in host adaptation for diverse pathogens. EA promotes growth and influences virulence during host infection. Although EA utilization genes have been identified in diverse bacteria (nonpathogenic and pathogenic), a prevailing idea is that commensal bacteria do not utilize EA to enhance growth, and thus, EA is a noncompetitive metabolite for pathogens. Here, we show that EA augments growth of two human commensal strains of *Escherichia coli*. Significantly, these commensal strains grow more rapidly than, and even outcompete, the pathogen EHEC specifically when EA is provided as the sole nitrogen source. Moreover, EA metabolism-independent gene expression is similarly conserved in the human commensal *E. coli* strain HS and influences expression of adhesins. These findings suggest a more extensive role for EA utilization in bacterial physiology and host-microbiota-pathogen interactions than previously appreciated.

## Introduction

The microbiota plays essential roles in human health. For example, the microbiota functions as a barrier against invading pathogens by limiting access to nutrients (97). Significantly, bacterial pathogens have evolved to exploit specific host- and microbiota-derived metabolites to sidestep nutritional competition and control expression of virulence traits (97). EA utilization plays a central role in host adaptation for a diverse range of pathogens, including opportunistic pathogens (98, 99). EA can serve as a carbon, nitrogen, and/or energy source to promote growth as well as a signal to influence virulence during host infection (73, 82, 85-87, 89, 90). In the *Enterobacteriaceae*, EutR senses EA and AdoCbl to directly activate *eut* transcription (79, 81). Moreover, in the foodborne pathogens EHEC and *Salmonella enterica* serovar Typhimurium, EutR regulates expression of virulence traits (81, 86, 88, 91). Despite the continual replenishment of EA in the GI tract, it has been reported that commensal bacteria do not utilize EA (84), and thus, EA utilization is a trait associated with pathogenesis (98, 99).

## Results

### EA supports the growth of commensal *E. coli*

The idea that EA is a noncompetitive metabolite for pathogens is largely perpetuated by data that showed that commensal *E. coli* isolated from ruminants did not consume EA in a modified bovine intestinal fluid (84). However, subsequent genome sequencing revealed that at least one of the *E. coli* strains used in the study contained several single nucleotide polymorphisms (SNPs) and an insertion element in the *eut* operon (100), which is expected to render this strain unable to utilize EA. In contrast, the *eut* operon of the human commensal *E. coli* HS strain contains an intact *eut* operon (21). HS was isolated from the stool of a healthy laboratory scientist and

is used as a representative of nondomesticated *E. coli* in a number of human colonization studies (19-21). Therefore, to revisit EA utilization by human commensal *E. coli*, we assessed growth of HS when cultured in a minimal medium containing EA as the sole nitrogen or carbon source. Physiologically relevant concentrations of EA supported EutR-dependent growth of HS when provided as a nitrogen (but not carbon) source (Fig. 2-1A to C). Similar to other *E. coli* strains, growth on EA required the addition of AdoCbl (Fig. 2-1C).

#### EA promotes the growth of commensal *E. coli* in the presence of other nitrogen sources

The GI tract contains several nitrogen sources that might diminish the potential importance of EA utilization in HS. To test this, we measured growth of HS in minimal medium containing NH<sub>4</sub> only or NH<sub>4</sub> and EA. When EA was added as a supplement to the medium, HS grew to a higher cell density than it did in medium containing only NH<sub>4</sub> (Fig. 2-1D). In support of these data, we also measured a significant increase in *eut* gene expression from HS grown in medium supplemented with EA compared to medium without EA supplementation (minimal medium containing NH<sub>4</sub> or Dulbecco's modified Eagle's medium) (Fig. 2-1E; see also Fig. 2-2). To confirm that EA utilization by a human *E. coli* isolate was not unique to the HS isolate, we next examined EA utilization in *E. coli* Nissle, which was isolated from the stool of a German soldier during World War I (22, 23). Consistent with the HS data, Nissle grew and responded to EA (Fig. 2-3A to D). Altogether, these data indicate that human commensal *E. coli* strains have maintained the ability to sense and utilize EA as a metabolite and that EA enhances growth in the presence of alternative nitrogen sources (as would be found in the gut).

### EA alters commensal fimbrial gene expression

We previously reported that EA influences the expression of genes carried outside the *eut* operon in EHEC and *Salmonella*, including expression of fimbriae (81, 86, 88, 91). HS and EHEC share a conserved set of fimbrial loci; therefore, we next measured expression of one gene in each of the conserved loci (expression of eight genes was measured) in HS grown in minimal medium with NH<sub>4</sub> only or NH<sub>4</sub> and EA. We measured a ~2- and 3-fold change in expression of genes carried in the *yad* and *ybg* loci, respectively (Fig. 2-1F). Interestingly, EA supplementation resulted in reduced levels of fimbrial gene expression in HS, which is the opposite of the impact of EA on EHEC fimbrial gene expression. These differences in expression may be reflective of the different colonization niches of these strains (lumen/mucus [HS] versus epithelial attachment [EHEC]). Regardless, these findings provide proof-of-principle data that similarly to EA-dependent growth, sensing EA to alter metabolism-independent gene expression is conserved in human commensal *E. coli* and not restricted to pathogens.

### Commensal *E. coli* outcompete EHEC during growth using EA

Scavenging nutrients is paramount for success in colonizing the host intestinal niche (101, 102). Commensal *E. coli* and EHEC compete for similar resources (101), and EA has been proposed to provide a selective growth advantage to EHEC over commensal *E. coli* (84). Therefore, we next compared growth of HS and EHEC in EA-minimal medium (containing glucose as the carbon source). Surprisingly, HS grew more rapidly than EHEC when EA was provided as the sole nitrogen source (Fig. 2-4A), with a doubling time of 1.6 h compared to 4.3 h, respectively (of note, the doubling time of Nissle was 1.3 h [Fig. 2-3A]). Consistent with these data, during competition HS was recovered at nearly 10-fold-higher levels than EHEC (Fig. 2-4B). *eut* expression and/or enzymatic

activity may be subject to carbon catabolite repression (63, 103); therefore, it is possible that effectiveness of carbon catabolite repression between HS and EHEC caused the differences in growth rates. To test this idea, we repeated the growth and competition experiments in EA-minimal medium containing glycerol as the sole carbon source. During exponential growth, growth rates of HS and EHEC were similar to growth rates in medium containing glucose, with doubling times of 1.4 h and 4.2 h, respectively (Fig. 2-4C). Of note, we observed a slightly shorter lag phase for EHEC grown in EA-minimal medium containing glycerol compared to glucose. Even so, consistent with the previous assay, HS was recovered in higher numbers than EHEC during competition (>2-fold) (Fig. 2-4D). Interestingly, this growth advantage was specific for EA utilization as no differences in bacterial growth or recovery were measured when HS and EHEC were cultured in minimal medium containing NH<sub>4</sub> as the sole nitrogen source (Fig. 2-4E and F and Fig. 2-5A and B).

## **Discussion and Future Directions**

Although genes encoding EA utilization proteins are carried by phylogenetically diverse bacteria (63), EA utilization has been suggested to be a potential virulence determinant and/or has been specifically linked to pathogenesis (i.e., references (85, 99, 104-107)). Our findings reveal that commensal GI bacteria rely on EA to enhance growth, and thus, EA utilization is more complex than previously appreciated.

Questions remain to elucidate EA metabolism by *E. coli*. *E. coli* grow using EA as a source of nitrogen and carbon (84, 108); however, *E. coli* metabolism of EA as a carbon source is incompletely understood. A minimal nutrient medium for *E. coli* is composed of organic components (a source each of carbon, nitrogen, and phosphorus) and inorganic salts, which together provide the minimal growth requirements for *E. coli* (109). In a

minimal medium containing glucose as a carbon source and EA as the sole nitrogen source, *E. coli* grows under aerobic conditions (84), demonstrating that EA supports *E. coli* growth as a nitrogen source. In contrast, EA does not support the growth of *E. coli* in minimal medium containing ammonium as a nitrogen source and EA as the sole carbon source (84, 108). A recent study using uropathogenic *E. coli* (UPEC) was the first to demonstrate that *E. coli* grows using EA as a carbon source (108). For these experiments, they grew UPEC strains in an artificial urine medium (AUM) with supplemental EA. AUM is a defined medium that contains multiple nitrogen sources (urea and ammonia) and carbon sources (amino acids, lactate, and citrate) (110). Following EutBC breakdown of EA into ammonia and acetaldehyde, EutE catalyzes the breakdown of acetaldehyde to the carbon source acetyl-CoA. Acetyl-CoA can enter the TCA cycle coupled with oxidative phosphorylation to generate ATP (74); therefore, a  $\Delta eutE$  strain is unable to use EA as a source of carbon (but grows at a comparable rate to WT using EA as a sole nitrogen source in minimal media (108)). Comparison of growth of  $\Delta eutE$  to WT in AUM with added EA, therefore, allowed the authors to specifically evaluate whether EA augments the growth of *E. coli* when used as a carbon source. A  $\Delta eutE$  strain had impaired growth compared to WT in AUM with added EA (108). These data suggest that *E. coli* metabolize EA as a carbon source to boost growth. Five *eut* operon proteins form the structural components of a microcompartment to increase the local concentration of enzymes required for EA metabolism and contain the toxic intermediate acetaldehyde (70). Notably, EA promotes the formation of microcompartments that are visible by transmission electron microscopy (TEM) in the majority of *E. coli* cells grown in AUM with 10 mM EA, while a minority of *E. coli* cells grown in minimal medium with 10 mM EA generated microcompartments (108). Further work is needed to determine how AUM supports EA

metabolism as a carbon source. Expression of the 17-gene *eut* operon is energetically costly, and this study suggests that a minimal nutrient medium containing EA as the sole carbon source does not provide sufficient energy to support robust microcompartment formation and subsequent carbon metabolism. Only EutBC expression is required to promote EA metabolism as a nitrogen source; therefore, it is unsurprising that *E. coli* grows using EA as a source of nitrogen in minimal medium. A minimal medium also does not recapitulate the abundant nutrient sources available in the intestinal tract. We hypothesize that AUM supports *E. coli* EA metabolism as a carbon source by providing additional sources of carbon to support the energetic cost of *eut* gene expression. First, we would test growth of HS using EA as a carbon source in AUM to ensure that this ability is not specific to UPEC. To test our hypothesis, we could evaluate growth of WT compared to  $\Delta eutE$  HS in minimal medium containing EA with the addition of individual supplemental carbon sources. If multiple carbon sources support *E. coli* EA metabolism as a carbon source, then this would support our hypothesis. Alternatively, if other carbon sources did not support *E. coli* EA metabolism as a carbon source, then specific component(s) of AUM are promoting EA metabolism by an unknown mechanism; to further investigate, we would add AUM components individually and in combination to gain information as to how this media contributes to EA metabolism. These studies would expand understanding of what conditions support EA metabolism.

EA affects metabolism-independent gene expression in both pathogenic (81, 88, 91) and commensal *E. coli* (Fig. 2-1F). Since EutR and ~2,200 genes are conserved among strains of *E. coli* (21), EutR in EHEC and commensal *E. coli* may share regulatory targets. In EHEC, EA promotes EutR and EutR-independent mechanisms that regulate fimbrial gene expression (91); therefore, EA alters fimbrial gene expression in commensal *E. coli* by one or both of these strategies. To test EutR-dependent gene expression, we

would generate  $\Delta eutR$  mutants in HS and Nissle and perform targeted evaluation of fimbrial gene expression in  $\Delta eutR$  and WT grown in the absence and presence of EA. If fimbrial gene expression is regulated by EA through mechanisms independent of EutR, then this would suggest that both EHEC and commensal *E. coli* encode alternate EA sensors that modulate gene expression. If our data lead in this direction, we can identify additional EA binding partners (in both commensal *E. coli* and EHEC) using mass spectrometry techniques (111). If EutR regulates fimbrial gene expression in commensal *E. coli*, then EutR-dependent gene regulation independent of metabolism extends to commensal *E. coli*. We can further elucidate the effect of EutR on gene expression through RNA-seq and compare direct binding targets of EHEC and HS EutR using ChIP-seq. These studies would reveal the extent of conservation in EutR-dependent gene regulation and other EA sensing mechanisms among commensal *E. coli* and EHEC.

Additional future studies will extend these findings into the intestinal environment to understand whether commensal *E. coli* EA metabolism disrupts pathogen infection. Commensal *E. coli* may outgrow pathogens in the intestinal tract using EA, as our growth data in co-culture with EHEC suggest (Fig. 2-4). This may lead to impaired EHEC colonization. To test this hypothesis, we would pre-colonize gnotobiotic mice with WT or  $\Delta eutB$  HS and then infect mice via oral gavage with WT *Citrobacter rodentium*, a murine model of EHEC infection. If WT but not  $\Delta eutB$  HS inhibits *C. rodentium* colonization levels, then EA metabolism by commensal *E. coli* contributes to nutritional colonization resistance against pathogenic infection. Alternatively, since EA has been measured at high levels in the intestinal tract (87), it is possible that EA is a noncompetitive metabolite for both pathogens and the microbiota.

Overall, this work suggests that further investigation on the impact of EA utilization in intestinal microbiota-pathogen interactions is warranted.

## Materials and Methods

### Strains, plasmids, and recombinant DNA

Strains used in the study are described in Table 1. Bacteria were grown overnight (O/N) shaking in Luria-Bertani (LB) at 37°C. For growth curves, O/N cultures were washed and resuspended in PBS and then diluted 1:100 into the indicated growth medium. M9 minimal medium (109) was prepared without the addition of a nitrogen source to the minimal salts as previously described (88). Briefly, this medium (1 L) was made by adding 200 mL of concentrated M9 salts (containing per liter: 64 g Na<sub>2</sub>HPO<sub>4</sub>·7H<sub>2</sub>O; 15 g KH<sub>2</sub>PO<sub>4</sub>; 2.5 g NaCl); 2 mL 1 M MgSO<sub>4</sub>, 100 µl 1 M CaCl<sub>2</sub>, and 5 mg thiamine. Glucose was typically added as the carbon source (0.4% final concentration). When indicated, glycerol was added as the carbon source (0.4% final concentration). The nitrogen sources (Sigma) were EA hydrochloride and NH<sub>4</sub>Cl. Dulbecco's Modified Eagle Medium was purchased from Invitrogen. Unless indicated, 150 nM AdoCbl was added to the medium whenever EA was added (Sigma).

An *eutR* deletion strain of *E. coli* HS (strain designation: MK85) was generated using  $\lambda$ -red mutagenesis (112). Briefly, PCR products (using primers listed in Table 2) were amplified from plasmid pKD4 with flanking regions matching *eutR* and transformed into *E. coli* HS expressing the Red genes from plasmid pKD46. The resistance cassette was resolved with flippase from temperature-sensitive plasmid pCP20, which was subsequently cured by growing at 42°C. The deletion was confirmed by sequencing. The  $\Delta$ *eutR* mutant was complemented with plasmid pCAR001. pCAR001 was constructed by amplifying *E. coli* HS genomic DNA using primers specific to the *eutR* gene, including 206 nucleotides upstream of the ATG start site (using primers listed in Table 2). Amplified DNA

was digested with NheI and SacI and inserted into pGENMCS (113) (Addgene MTA). As a control, the WT and  $\Delta eutR$  strains were transformed with the empty pGEN-MCS vector.

### Growth and competition experiments

Bacteria were grown aerobically in minimal medium with 5 mM EA or 5 mM NH<sub>4</sub>Cl, unless otherwise indicated. Doubling time was calculated as  $\ln(2) / \text{growth rate}$  during linear growth phase. For competition experiments, equal numbers of bacterial colony forming units (CFU) were added to minimal medium supplemented with EA or NH<sub>4</sub>Cl. For glucose cultures, samples were collected at 25 h (EA) or 3.5 h (NH<sub>4</sub>Cl), time points that were reflective of EHEC at mid-log growth phase as determined by pure culture growth curves. For glycerol cultures, samples were collected at 8.75 (EA) or 6 h (NH<sub>4</sub>Cl). Samples were serially diluted and plated on LB with no selection to enumerate total CFU or LB with streptomycin to enumerate EHEC CFU. *E. coli* HS CFU were determined by subtracting EHEC CFU from total CFU. The competitive index was calculated by dividing *E. coli* HS by EHEC CFU.

### RNA extraction and RT-qPCR

Bacteria were grown in DMEM for 6 h statically under a 5% CO<sub>2</sub> atmosphere without or with EA supplementation (5 mM) or aerobically in minimal medium containing 2 mM NH<sub>4</sub>Cl or 2 mM NH<sub>4</sub>Cl and 5 mM EA to an O.D.<sub>600</sub> of 0.3-0.4. Then bacterial cells were suspended in Trizol (Life Technologies), and RNA was extracted using the RiboPure Bacteria RNA isolation kit (Ambion). Primers used in real-time RT-qPCR assays were validated prior to use and are listed in Table 2. Reaction mixtures were prepared as previously described (114). RT-qPCR was performed using a one-step reaction in an ABI 7500-FAST sequence detection system (Applied Biosciences). All data were normalized

to the levels of *rpoA* and analyzed using the comparative cycle threshold (CT) method (115).

### Statistical analyses

For growth curves and gene expression experiments, statistical significance was determined using Student's t test, and a P value of  $\leq 0.05$  was considered significant. For the competition experiments, statistical significance was determined by one-sample t test with an expected value of 1. All experiments were repeated at least twice and with three biological replicates.

## Figures

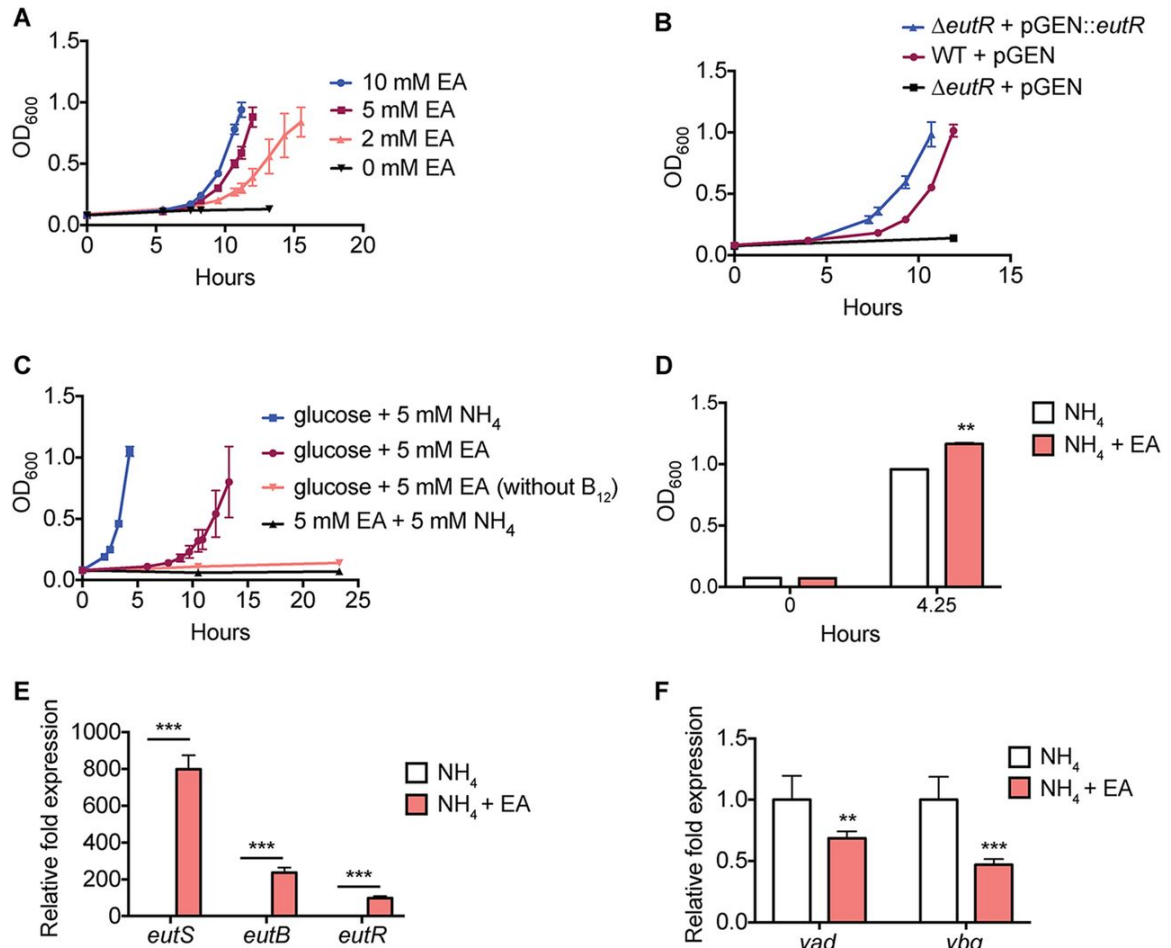


**Fig. 2-1. EA-dependent growth and gene expression in *E. coli* HS.** (A) Growth curve of HS grown in minimal medium with glucose as a carbon source and EA as the sole nitrogen source at indicated concentrations.  $n = 3$ . OD<sub>600</sub>, optical density at 600 nm. (B) Growth curve of wild type (WT) with empty vector,  $\Delta*eutR*$  mutant with empty vector, and *eutR* complemented strain grown in minimal medium containing EA.  $n = 3$ . (C) Growth curve of HS grown in minimal medium with indicated carbon and nitrogen sources or without AdoCbl, as specifically indicated.  $n = 3$ . (D) Bacterial cell density at indicated time points after growth in minimal medium with NH<sub>4</sub> or NH<sub>4</sub> and EA.  $n = 3$ . (E) Reverse transcription-quantitative PCR (RT-qPCR) of *eut* gene expression in HS grown in in

minimal medium with  $\text{NH}_4$  or  $\text{NH}_4$  and EA.  $n = 3$ . (F) RT-qPCR of fimbrial genes in HS grown in minimal medium with  $\text{NH}_4$  or  $\text{NH}_4$  and EA.  $n = 6$ . For all, unless indicated, AdoCbl was added whenever the medium was supplemented with EA. Error bars represent the mean  $\pm$  standard deviation (SD). \*\*,  $P \leq 0.01$ ; \*\*\*,  $P < 0.001$ .

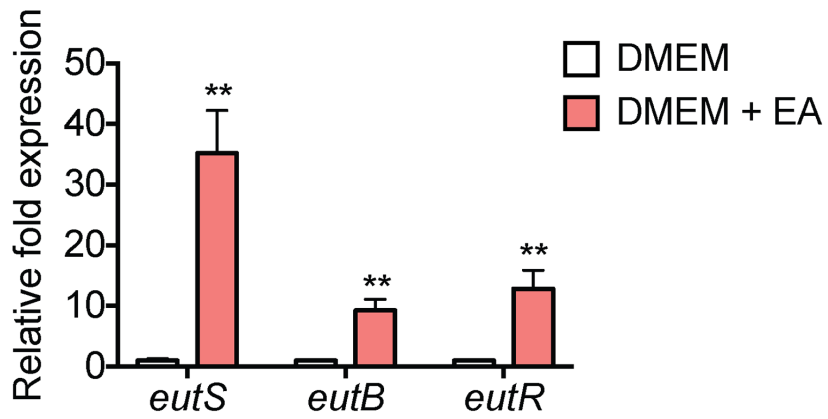


**Fig. 2-2. EA promotes HS *eut* gene expression in a defined medium.** RT-qPCR of *eut* gene expression in *E. coli* HS grown in Dulbecco's modified Eagle's medium (DMEM) without or with EA and AdoCbl.  $n = 3$ ; error bars represent the mean  $\pm$  SD. \*\*,  $P < 0.01$ .

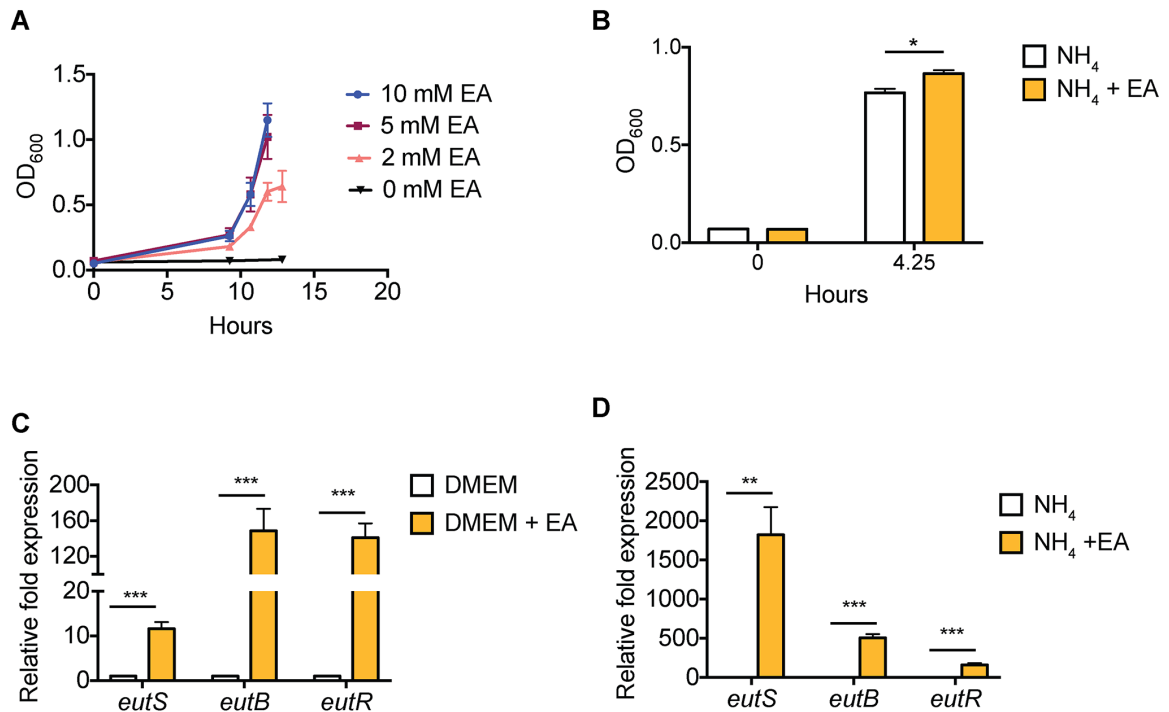


**Fig. 2-3. EA promotes growth and gene expression in *E. coli* Nissle.** (A) Growth curve of Nissle grown in minimal medium with glucose as the carbon source and EA as the sole nitrogen source at indicated concentrations and AdoCbl. (B) Bacterial cell density at indicated time points after growth in minimal medium with NH<sub>4</sub> or with NH<sub>4</sub>, EA, and AdoCbl. (C) RT-qPCR of *eut* gene expression in Nissle grown in DMEM without or with EA and AdoCbl. (D) RT-qPCR of *eut* gene expression in Nissle grown in minimal medium containing NH<sub>4</sub> or EA and AdoCbl. For all, *n* equals 3; error bars represent the mean ± SD. \*, *P* < 0.05; \*\*, *P* ≤ 0.01; \*\*\*, *P* ≤ 0.001.

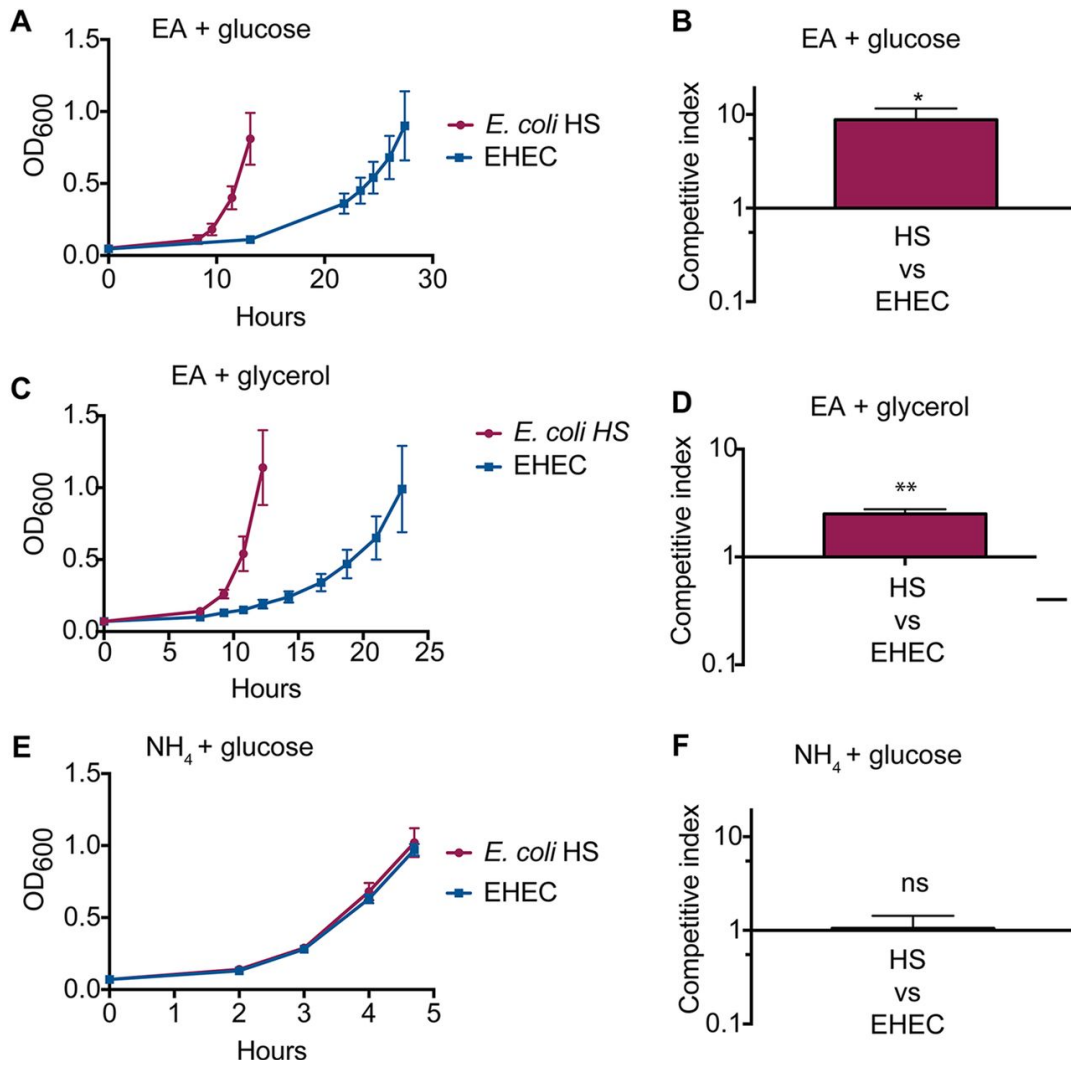


**Fig. 2-4. HS outcompetes EHEC specifically during growth on EA.** (A) Growth curve of *E. coli* HS and EHEC in minimal medium with EA and glucose. (B) Competition assay between *E. coli* HS and EHEC in minimal medium with EA and glucose. (C) Growth curve of *E. coli* HS and EHEC in minimal medium with EA and glycerol. (D) Competition assay between *E. coli* HS and EHEC in minimal medium with EA and glycerol. For panels A to D, AdoCbl was added to the medium. (E) Growth curve of *E. coli* HS and EHEC in minimal medium with NH<sub>4</sub> and glucose. (F) Competition assay between *E. coli* HS and EHEC in

minimal medium with  $\text{NH}_4$  and glucose. For all,  $n$  equals 3; error bars represent the mean  $\pm$  standard deviation. \*,  $P \leq 0.05$ ; \*\*,  $P \leq 0.01$ ; ns,  $P > 0.05$ .

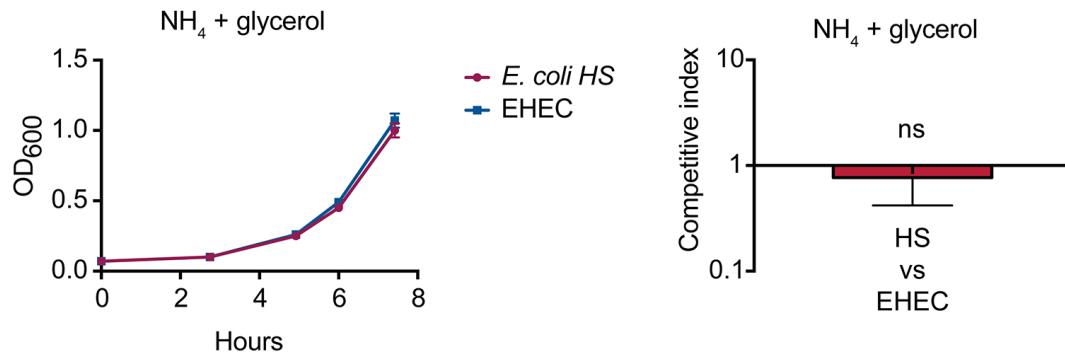


**Fig. 2-5. HS and EHEC grow at similar rates using glycerol.** (A) Growth curve of *E. coli* HS and EHEC in minimal medium with NH<sub>4</sub> and glycerol. (B) Competition assay between *E. coli* HS and EHEC in minimal medium with NH<sub>4</sub> and glycerol. For all,  $n$  equals 3; error bars represent the mean  $\pm$  SD. ns,  $P > 0.05$ .

**Chapter 3: *Citrobacter rodentium* ethanolamine utilization contributes to intestinal virulence, colonization, and transmission**

Part of this chapter has been adapted from “The ethanolamine-sensing transcription factor EutR promotes virulence and transmission during intestinal infection.”  
Carol A. Rowley and Melissa M. Kendall. 2020. Under review.

## Abstract

EHEC is an important foodborne pathogen that causes significant morbidity and mortality in developed countries. Young children are at a heightened risk of severe complications from EHEC infection, including acute renal failure due to HUS. EHEC is classically transmitted through ingestion of contaminated food products, but direct person-to-person transmission is the most common route of infection among young children. Enteric pathogens have evolved strategies to sense their environment and alter gene regulation to promote effective colonization, which likely impacts transmission to naïve hosts, though this area is vastly understudied. EHEC has evolved to sense the metabolite EA through the transcription factor EutR to promote virulence gene expression. Because EHEC mouse infections do not recapitulate pathogenesis, we used the murine model of EHEC infection, *C. rodentium*, to examine the role of EutR in pathogenesis. EutR promotes growth using EA and regulates virulence gene expression in *C. rodentium*; therefore, *C. rodentium* recapitulates EutR-dependent gene regulation in EHEC. We determined that passage through the intestinal environment enhances EutR expression. Additionally, we measured impaired virulence factor expression and a lower bacterial burden of  $\Delta eutR$  shed in stool compared to WT. Furthermore, the  $\Delta eutR$  strain was transmitted at lower rates to naïve mice compared to WT. Together, these data demonstrate a critical role for EutR in coordinating both niche adaptation to promote colonization and transmission to new hosts.

## Introduction

Transmission of EHEC is classically associated with ingestion of foodborne sources but also occurs through fecal-oral transmission. Cattle are often colonized with EHEC; therefore, beef and other foods contaminated by bovine feces, such as romaine lettuce, are common sources of infection (116). It is less well-appreciated, however, that direct fecal-oral person-to-person transmission causes a substantial proportion of EHEC infections (10-15%)(28, 29), especially in vulnerable populations. Person-to-person transmission is the leading route of infection among children under the age of 5 years (117), and outbreaks are commonly associated with daycare centers (28, 118). Outbreaks in young children are especially concerning because this population sheds EHEC significantly longer than adults and is at a heightened risk of severe disease (119). Additionally, person-to-person transmission has been implicated in an EHEC outbreak in a facility for individuals with intellectual disabilities, potentially driven by impaired personal hygiene (120). Therefore, person-to-person transmission of EHEC is an important route of infection to further investigate.

The propagation of EHEC in a host population is largely determined by its ability to colonize a host niche and to efficiently transmit to naïve hosts. EutR regulates metabolism and virulence in EHEC (67, 121, 122) through sensing EA. In *Salmonella* Typhimurium, EutR promotes intestinal colonization (86, 87) and survival in macrophages (86). In EHEC, EutR regulates virulence factor expression and promotes adhesion to epithelial cells and AE lesion formation (81, 88, 91). Conserved virulence factors contribute to the success of mouse colonization (48, 57) and transmission (123) of *C. rodentium*, an AE pathogen and murine model of EHEC infection.

In this study, we investigate the role of EutR in virulence gene regulation during host infection using *C. rodentium*. We demonstrate that EutR promotes the virulence, bacterial

burden, and the ability of *C. rodentium* to effectively transmit to naïve hosts. Overall, these data support a critical role for this conserved transcriptional regulator in enteric pathogenesis.

## Results

### EA supports EutR-dependent *eut* gene expression and EA metabolism in *C. rodentium*

*C. rodentium* encodes an *eut* operon that is conserved among Enterobacteriaceae (Fig. 3-1A). In Enterobacteriaceae, the *eut* operon is transcriptionally regulated by EutR (81) and encodes proteins that are required for EA metabolism (84). The EutR protein in *C. rodentium* shares 92% amino acid conservation with the EHEC EutR protein, with 96.3% sequence similarity, according to an alignment using EMBOSS Needle (Fig. 3-1B). In EHEC, EutR binds to the P1 promoter region upstream of *eutS* (Fig. 3-1A, referred to as the “*eutS* promoter”) to directly regulate *eut* gene expression (81). The *eutS* promoter region is also highly conserved between EHEC and *C. rodentium*, with 100% conservation of the predicted Enterobacteriaceae EutR binding region (63) (Fig. 3-1C, with the conserved Enterobacteriaceae binding region highlighted in yellow). We predicted that EutR directly binds the *eutS* promoter in *C. rodentium* to regulate *eut* gene expression and to promote EA metabolism. To test the effect of EutR on *C. rodentium* *eut* expression, we grew WT and  $\Delta$ *eutR* without or with EA supplementation and extracted RNA. We determined that EA promoted *eutS* gene expression in WT but not  $\Delta$ *eutR* (Fig. 3-1D). Furthermore, a defect in *eutS* expression in the  $\Delta$ *eutR* strain grown with EA was restored through *eutR* complementation (Fig. 3-1E). To evaluate EutR binding to the *eutS* promoter, we performed *in vivo* chromatin immunoprecipitation (ChIP) by expressing EutR-MBP or MBP from a plasmid in the  $\Delta$ *eutR* strain. We immunoprecipitated EutR-MBP

and associated DNA, determined the fold enrichment of the *eutS* promoter DNA compared to fragmented input DNA, and normalized the fold enrichment to enrichment by MBP. We measured 4-5-fold enrichment of the *eutS* promoter DNA following EutR-MBP immunoprecipitation by qPCR, normalized to MBP (Fig. 3-1F). These data demonstrate that EutR directly binds to the *eutS* promoter. Finally, we showed that *C. rodentium* grows using EA as a nitrogen source and that a growth defect in  $\Delta$ *eutR* using EA can be complemented through plasmid-based expression of *eutR* (Fig. 3-1G). The growth defect of  $\Delta$ *eutR* is specific to growth using EA (Fig. 3-1H). These data demonstrate that *C. rodentium* EutR senses EA to promote *eut* gene expression and EA-dependent growth.

#### EutR promotes *C. rodentium* virulence gene expression

In EHEC, EutR enhances the expression of virulence factors, including fimbriae, the T3SS machinery and effectors (81, 88, 91) and promotes attachment to epithelial cells and formation of AE lesions (88, 91). However, *in vivo* studies are lacking to fully understand the impact of EutR on EHEC pathogenesis. Therefore, in this study, we evaluated the effect of EutR on host-pathogen interactions using the murine model *C. rodentium* (49, 51, 52, 124). *C. rodentium* encodes a LEE pathogenicity island that is conserved with EHEC (Fig. 3-2A) and regulated by Ler (47).

First, we evaluated the impact of EutR on *C. rodentium* virulence gene expression *in vitro*. We grew WT and  $\Delta$ *eutR* in medium without or with EA supplementation, extracted RNA, and performed RT-qPCR. The expression of LEE-encoded *espA*, which encodes the T3SS filament, was increased in WT grown with the addition of EA, whereas *espA* expression in  $\Delta$ *eutR* was unchanged with the addition of EA (Fig. 3-2B). These data show that EutR senses EA to promote *espA* expression. Additionally, plasmid-based expression

of *eutR* rescued a defect in *espA* and *ler* expression in the  $\Delta$ *eutR* strain compared to WT (Fig. 3-2C). Using RNA extracted from WT and  $\Delta$ *eutR* grown with EA, we also evaluated the expression the LEE-encoded translocated intimin receptor (*tir*) and genes that are not directly regulated by Ler, including non-LEE encoded T3SS effectors and *regA*, which encodes a virulence regulator that promotes LEE expression (40, 50, 125-128). We measured decreased expression of each gene in  $\Delta$ *eutR* compared to WT (Fig. 3-2D), suggesting that EutR affects the expression of multiple virulence genes in *C. rodentium*. EHEC encodes proximal and distal *ler* promoters, and EutR directly binds to the proximal Ler promoter to regulate virulence gene expression (81). However, *C. rodentium* shares a conserved distal *ler* promoter region with EHEC (Fig 3-2E) but does not encode the proximal *ler* promoter (129). To investigate if EutR directly binds to the *ler* promoter in *C. rodentium*, we performed CHIP-qPCR and measured a 1.5-fold enrichment of the *ler* promoter compared to fragmented input DNA and normalized to MBP (Fig. 3-2F). Importantly, we did not measure enrichment of the negative control housekeeping gene *rpoA* (Fig. 3-2F). These data suggest that EutR directly and specifically binds to the *ler* promoter. In a complementary study, we purified the EutR-MBP and MBP proteins and performed electrophoretic mobility shift assays (EMSAs) to test direct binding of the EutR protein to biotinylated probes encoding the promoter regions of *ler*, *regA*, and negative control *bla* (ampicillin gene). When increasing concentrations of EutR were incubated with each probe, a shift in the detected size of the *ler* promoter probe was observed. These data suggest that EutR bound to the *ler* promoter. However, the *regA* and *bla* promoter probes did not shift in size when EutR was added, suggesting that EutR does not bind these promoters (Fig. 3-2G). Additionally, MBP alone did not shift the *ler* promoter probe, demonstrating that EutR (not MBP) specifically binds the *ler* probe (Fig. 3-3). These data

demonstrate that EutR binds distinct promoter regions of *ler* in EHEC and *C. rodentium* that result in conserved effects on LEE gene expression. Overall, EutR directly regulates *ler* expression in *C. rodentium* to impact virulence gene expression.

#### *C. rodentium* shedding, EA measurements, and *eutR* expression over time

Following inoculation by oral gavage, *C. rodentium* has an early tropism for the cecal patch and colonizes the colon at high levels by five days post infection (130). For our studies, we infected C57BL/6J mice with *C. rodentium* via oral gavage using strain DBS100 (54), as previously described (49, 51, 52, 124). Because DBS100 lacks antibiotic resistance to allow reliable enumeration of bacterial colony forming units (CFU) shed in stool at low levels, only unresolved strains that encode an antibiotic resistance cassette were used during infection. An unresolved  $\Delta lacZ$  strain was used as the “WT” strain in all animal infections, which is enumerated from stool at indistinguishable levels from DBS100 (Fig. 3-4). Following infection with WT *C. rodentium*, we enumerated CFU shed in stool at multiple time points to learn about our experimental system. *C. rodentium* was shed at increasing levels until reaching maximum shedding levels at 10 dpi and beginning to clear around 16 dpi (Fig. 3-5A).

Intestinal EA levels can be altered by enteric infection (87, 131), and EA promotes EutR-dependent gene expression ((81, 88); Fig. 3-1D-E); therefore, we tested whether EA levels change during *C. rodentium* infection. We infected or mock-infected with WT *C. rodentium* or PBS, respectively, and quantified EA levels from the colon. We measured similar EA concentrations in the colon following WT infection at 6 and 14 dpi compared to mock-infection (Fig. 3-5B). Therefore, *C. rodentium* infection does not affect EA concentrations in the colon at 6 and 14 dpi.

To determine time points of interest for our studies, we evaluated *eutR* expression over the course of infection. For these studies, we used a bioluminescent transcriptional reporter strain, which contains a plasmid encoding the *eutR* promoter upstream of bacterial luciferase genes in a WT background (Fig. 3-5C). We infected mice with this strain and monitored expression of *eutR* shed in stool compared to expression during *in vitro* growth. *eutR* expression was enhanced 5-10-fold *in vivo* compared to *in vitro* growth throughout infection (Fig. 3-5D), suggesting that the intestinal environment enhances *eutR* expression. *eutR* expression levels and EA concentrations are similar at multiple time points we examined; therefore, we evaluated EutR-dependent virulence gene expression at 10 dpi, a time point at which we measured *eutR* expression and a high bacterial burden.

#### EutR promotes the virulence gene expression of *C. rodentium* during colonic infection

Expression of the LEE results in *C. rodentium* T3SS formation at the epithelial layer of the colon and subsequent AE lesion formation (51). Because EutR directly regulates *ler* expression, which is the master LEE regulator, we first evaluated EutR-dependent virulence gene expression in *C. rodentium* during infection. We infected mice with WT or  $\Delta$ *eutR*, harvested colonic tissue at 10 dpi, and removed luminal contents. We performed RT-qPCR to evaluate *ler* expression normalized to *C. rodentium* 16S rRNA. We measured significantly lower *ler* expression in  $\Delta$ *eutR* in the colon compared to WT (Fig. 3-6A). Additionally, we examined the expression of fimbrial gene *kfcC*, which is highly upregulated *in vivo* (but undetectable *in vitro*) (132) and contributes to *C. rodentium* colonization (126). Expression of *kfcC* was also decreased in  $\Delta$ *eutR* in the colon compared to WT (Fig. 3-6B).

In complementary studies, we used a transcriptional reporter to evaluate *ler* expression *in vivo*. First, we constructed a transcriptional reporter strain that encodes the *ler* promoter upstream of bacterial luciferase genes on a plasmid (Fig. 3-6C). This plasmid is retained in *C. rodentium* shed in stool through 10 dpi (Fig. 3-7). At 10 dpi, we measured lower levels of *ler* expression in  $\Delta eutR$  compared to WT in the intestinal tract using an *in vivo* imaging system (IVIS) (representative images in Fig. 3-6D, quantified in 3-6E). The amplitude of the difference in *ler* expression between WT and  $\Delta eutR$  associated with colonic tissue was approximately 2-fold, whereas the IVIS-detected differences in *ler* expression was closer to 10-fold. We hypothesized that the total bacterial burden of *C. rodentium* was lower in  $\Delta eutR$  compared to WT and/or that EutR has an augmented effect on *ler* gene expression in the luminal contents, which were removed prior to gene expression analysis of *C. rodentium* in the colon. We begin to address these hypotheses in the following section, where we examine the virulence and colonization of luminal *C. rodentium* that is shed in stool.

#### EutR impacts the virulence gene expression and burden of *C. rodentium* shed in stool

Bacteria alter gene regulation in response to different intestinal microenvironments, such as the colonic epithelial layer and the lumen (133). The population of *C. rodentium* that proliferates in the colonic lumen is composed of bacteria that grow in the lumen without reaching the epithelial layer (134) in addition to bacteria that are shed from the epithelial layer into the lumen. Despite some bacteria in this niche never reaching the epithelial layer to form AE lesions, luminal *C. rodentium* that are shed in stool express *ler* during infection (57). Therefore, we evaluated whether EutR-dependent virulence gene regulation in *C. rodentium* in the colon is maintained in *C.*

*rodentium* shed in stool. To test this, we performed RT-qPCR to evaluate *ler* and *kfcC* expression in *C. rodentium* RNA extracted from stool. Similar to *C. rodentium* associated with colonic tissue, *ler* (Fig. 3-8A) and *kfcC* (Fig. 3-8B) expression were both a median of 2-fold lower in  $\Delta eutR$  compared to WT at 10 dpi, though *ler* expression differences did not reach statistical significance. To monitor *ler* expression in stool over time, we used the *ler* transcriptional reporter strain (Fig. 3-6C). At 2 dpi, the bacterial burden shed in stool was too low to accurately detect luminescence per CFU in most samples (Fig. 3-8C). At 4 and 6 dpi, *ler* expression per CFU was significantly lower in  $\Delta eutR$  shed in stool compared to WT (Fig. 3-8C). While  $\Delta eutR$  expressed a similar median 2-fold lower level of *ler* expression at 8 and 10 dpi, these results did not reach statistical significance. Overall, these results demonstrate that EutR promotes virulence gene expression in *C. rodentium* shed in stool.

To examine the impact of EutR on the burden of *C. rodentium* shed in stool, we infected mice with WT or  $\Delta eutR$  and monitored the bacterial burden over the course of infection. Similar CFU of WT and  $\Delta eutR$  were enumerated from stool at 2-6 dpi; however,  $\Delta eutR$  exhibited a defect in shedding burden compared to WT at 8 and 10 dpi, and this trend is also present on later days of infection (Fig. 3-8D). These data demonstrate that EutR-dependent gene expression alters bacterial shedding in stool by mid-infection.

#### EutR promotes *C. rodentium* transmission to naïve animals

*C. rodentium* that is shed in stool maintains *ler* expression throughout infection ((135); Fig. 3-8A,C), begging the question as to the role of virulence gene expression in shed *C. rodentium*. One explanation is that alterations in both the virulence gene expression and the bacterial burden shed in stool affect the transmission of *C. rodentium* to naïve hosts

(59, 123). Therefore, we hypothesized that EutR promotes *C. rodentium* virulence and burden shed in stool to enhance transmission to naïve hosts.

We examined the impact of EutR-dependent gene expression on transmission at two time points. At 6 dpi, WT and  $\Delta eutR$  are shed at similar levels (Fig. 3-8D), but we measured decreased virulence gene expression in  $\Delta eutR$  compared to WT (Fig. 3-8C). If EutR-dependent alterations in virulence factor expression impact transmission through mechanisms independent of bacterial burden, then we would expect  $\Delta eutR$  to transmit less effectively than WT at 6 dpi. To test this hypothesis, we infected “index” mice with WT or  $\Delta eutR$  and allowed infection to progress for 6 days. The bacterial burden and the virulence of index mice are reported in Fig. 9. At 6 dpi, each index mouse was cohoused with 3 naïve mice in a new cage with fresh bedding. Following 24 hours of cohousing, we separated the naïve mice into fresh individual caging (Fig. 3-10A). Naïve mice that were cohoused with 6 dpi index mice shed similar levels of *C. rodentium* at 2- and 4-days post exposure (Fig. 3-10B). These data show that EutR-dependent gene expression with a similar colonization burden at 6 dpi does not alter transmission to naïve hosts.

From here, we investigated the impact of EutR-dependent bacterial burden shed in stool on transmission at 10 dpi. The median bacterial burden of  $\Delta eutR$  at 10 dpi is below the level previously reported to promote effective transmission (59), while the burden of WT is above that level (Fig. 3-10C). If this difference in bacterial burden shed in stool is important for effective transmission, then we expect WT to more effectively transmit to naïve hosts than  $\Delta eutR$  at 10 dpi. To test this, at 10 dpi, we cohoused each index mouse with 3 naïve mice in a new cage with fresh bedding. Following 24 hours of cohousing, we separated the naïve mice from the index mice and placed them in caging with fresh bedding. In our initial experimental setup, we enumerated *C. rodentium* shed in feces at 2

days following exposure. Naïve mice cohoused with  $\Delta eutR$  index mice shed significantly lower burdens of *C. rodentium* in stool compared to mice cohoused with WT index mice (Fig. 3-10C), suggesting impaired initial transmission. *C. rodentium* is detected in the colon by 3 dpi (59); therefore, we repeated the experiment to monitor fecal shedding of *C. rodentium* up to 4 days post exposure. In agreement, mice cohoused with  $\Delta eutR$  index mice shed significantly lower levels of *C. rodentium* in stool compared to WT at 4 days post exposure (Fig. 3-10D). Overall, these data suggest that EutR significantly affects *C. rodentium* transmission, likely through the combined effects of altering virulence gene expression and altering the colonization burden shed in stool.

### Discussion and Future Directions

Ethanolamine is an important metabolite that affects the growth and pathogenesis of members of many bacterial families, including Enterobacteriaceae (98). EutR is central to EA utilization by Enterobacteriaceae, and it is important to understand how EutR expression is controlled in relevant host niches. Prior to this work, EutR expression from the *eutR* promoter (P2) had been measured *in vitro* at low constitutive levels (79). However, our data demonstrate that EutR expression from this promoter (Fig. 3-1A) is amplified following intestinal passage compared to *in vitro* growth (Fig 3-5D). These studies suggest that EutR expression is regulated by an unknown factor in the intestinal tract. The identification of additional factors that modulate EA-dependent gene regulation will have important implications for our understanding of pathogenesis.

Precise regulation of virulence gene expression is critical for a pathogen to colonize an intestinal niche and to transmit to naïve hosts (136, 137). The expression of Ler and fimbriae are important for the intestinal adaptation and colonization of AE

pathogens (33, 38, 47, 48, 50, 126, 138). We demonstrate that EutR directly regulates *ler* and alters *in vivo* expression of both *ler* and fimbriae *kfcC* (Fig. 3-6A-B, 3-8A-C). Subtle EutR-dependent alterations in gene expression may lead to changes in bacterial burden (Fig. 3-8D) that have amplified effects on the success of transmission and colonization of naïve hosts following transmission (Fig. 3-10C-D).

Virulence factors that contribute to *C. rodentium* colonization have been well-characterized, but the functional linkage among virulence, colonization, and transmission is rarely evaluated. A bacterial burden shed in stool of at least  $10^7 - 10^8$  CFU / g promotes effective fecal-oral transmission of *C. rodentium* between C57BL/6 animals (59). In our studies, the median burden of WT shed in stool at 10 dpi is at the level reported to promote transmission, while the median burden of  $\Delta$ *eutR* shed in stool is about 10-fold lower (Fig. 3-8D), below levels reported to support transmission. In agreement, we determined that EutR promotes transmission at 10 dpi (Fig. 3-10C-D). The evolutionary driving forces behind the bacterial acquisition of virulence genes have long been debated; the virulence trade-off hypothesis suggests that virulence traits evolved in pathogens specifically to promote optimal transmission success without killing the host (139). The trade-off hypothesis highlights the central role that transmission plays in pathogenesis. Despite the relevance of person-to-person transmission in EHEC outbreak settings (28, 118, 120), transmission remains an understudied area. In our study, we connect gene regulation by the transcription factor EutR with intestinal virulence, bacterial burden, and transmission success.

Future studies are needed to more fully understand the impact of EutR on host pathogenesis, including the effect of EA metabolism on *C. rodentium* colonization. We did not measure differences in EA levels during *C. rodentium* infection compared to mock-infection (Fig. 3-5B). These data may suggest that EA consumption is not occurring, as

EA levels decrease during *S. Typhimurium* infection due to EA metabolism (87). Intestinal inflammation did not change EA measurements during *S. Typhimurium* infection (87) but may increase EA levels during pathogenic *E. coli* infection (131), meaning that inflammatory changes could mask EA consumption *in vivo*. Therefore, the impact of EA metabolism on EA levels and the colonization of *C. rodentium* remains to be elucidated. To test the effect of EutR-dependent EA metabolism versus EutR-dependent gene regulation on colonization, we attempted to generate a metabolic mutant of *C. rodentium* that is unable to metabolize EA but retains EutR-dependent gene regulation (86, 88). EutBC is the EA-ammonia lyase that catalyzes the first step in EA metabolism (67, 76); therefore, deletion of *eutB* or *eutC* should result in a loss of EA metabolism while retaining *eutR* expression and EutR-dependent gene regulation (88, 140). We could then compete this strain with WT or  $\Delta$ *eutR* to determine the effect of EA metabolism on *C. rodentium* colonization. However, the  $\Delta$ *eutB* and  $\Delta$ *eutC* mutations in *C. rodentium* had polar effects on *eutR* expression and did not recapitulate EutR-dependent *eutS* or *espA* gene expression (Fig 3-11). As an alternative approach, we can delete smaller sections of either the *eutB* or *eutC* protein and/or introduce point mutations in catalytically important sites to avoid polar effects on *eutR* expression. Through these studies, we hope to determine the role of EA metabolism in *C. rodentium* colonization.

We have gained insight into EutR-dependent gene regulation and downstream effects on pathogenesis; however, ongoing studies will further mechanistically evaluate the role of EutR in AE pathogen gene regulation. Through targeted evaluation of gene expression, we determined that EutR directly regulates *ler* expression and alters the expression of additional virulence genes in *C. rodentium* that are not regulated by Ler (Fig. 3-2D). Furthermore, previous work has identified targets of EutR in EHEC (81, 88, 91).

ChIP-seq can be used to define and compare the EutR regulon in *C. rodentium* and EHEC. We performed targeted ChIP-qPCR to assess EutR targets in *C. rodentium* (Fig. 3-1F, 3-2F) using the EutR-MBP fusion protein and MBP as a control because we do not have an antibody against EutR. In these studies, we identified enrichment of *ler* and *eutS* promoter regions (Fig. 3-1F, 3-2F). In preliminary ChIP-seq studies, we did not identify many additional EutR binding targets of interest, possibly due to technical limitations. The MBP protein bound many DNA regions that EutR-MBP also binds, resulting in difficulty ascertaining enrichment of specific EutR binding sites. As an alternative approach, we can design a chromosomally FLAG epitope-tagged EutR protein expressed by a *C. rodentium* *eutR*<sup>FLAG</sup> strain and use an anti-Flag antibody to IP in the ChIP experiment (141). WT *C. rodentium* would be used alongside the *eutR*<sup>FLAG</sup> strain as a negative control to account for nonspecific binding of the anti-Flag antibody. Alongside ChIP studies, we would perform RNA-seq using WT and  $\Delta$ *eutR* *C. rodentium* and EHEC grown *in vitro* to elucidate EutR-dependent networks of gene expression. Additionally, we are currently performing experiments in which we infected mice with WT and  $\Delta$ *eutR* *C. rodentium*, harvested colons at 10 dpi, and are performing RNA-seq on *C. rodentium* in the colon and shed in stool. Through these studies, we hope to elucidate the relevance of pathways identified through ChIP-seq and *in vitro* RNA-seq to intestinal infection. From here, we can design genetic mutants in *C. rodentium* of identified targets in relevant metabolic and virulence pathways to determine what genes contribute to the EutR-dependent colonization and transmission phenotypes. We would first generate a  $\Delta$ *kfcC* mutant to compete with  $\Delta$ *eutR* and WT to elucidate the role of this fimbriae in EutR-dependent colonization; EutR promotes *kfcC* expression (Fig. 3-6B, 3-8B), and  $\Delta$ *kfcC* has a similar amplitude colonization defect to

*ΔeutR* (126). These studies will extend our understanding of EutR-dependent gene regulation in pathogenesis.

Virulence gene expression is critical for tissue colonization of the intestinal tract (48, 57, 135). We showed that EutR impacts the bacterial burden of *C. rodentium* shed in stool (Fig. 3-8D), but we did not determine the effect of EutR on *C. rodentium* in the colon, which contains tissue-associated bacteria. To test the hypothesis that EutR-dependent gene expression would lead to impaired colonization of *ΔeutR* compared to WT, we infected mice with WT or *ΔeutR* and harvested colonic tissue at 10 dpi. Luminal contents were removed from the colon, tissue was homogenized, and bacteria were enumerated by plating on selective media. In preliminary studies, *ΔeutR* was enumerated from the colon at a slightly lower median level in *ΔeutR* compared to WT (Fig. 3-12), and repeating these studies with higher numbers will determine the impact of EutR on colonization of *C. rodentium* in the colon. Additionally, further investigation is required to more carefully examine the effect of EutR on colonization at the epithelial layer and formation of AE lesions. Removing the luminal contents may not be sufficient to remove all non-tissue-associated bacteria to examine the burden of *C. rodentium* at the epithelium. EutR-dependent effects on colonization may apply to *C. rodentium* populations in the lumen and associated with colonic tissue or might primarily affect luminal *C. rodentium* that is shed in stool. We have performed preliminary experiments and validated that we can visualize tissue-associated *C. rodentium* via immunohistochemistry (IHC) using an anti-*E. coli* / *C. rodentium* antibody (Fig. 3-13)(142, 143). Using this technique, we can measure the effect of EutR on the burden of *C. rodentium* in the lumen, mucus layer, and at the epithelium. Furthermore, we can use transmission electron microscopy to directly examine the role of EutR on AE lesion formation on epithelial cells (144). Together, these studies will elucidate

the effect of EutR on colonic tissue colonization at the epithelium and AE lesion formation, two hallmarks of pathogenesis.

Passage through the intestinal tract promotes enteric pathogen virulence and transmission. A significantly lower infectious dose of both *C. rodentium* (123, 145) and enteric pathogen *Vibrio cholerae* (146, 147) is sufficient to cause infection with host-adapted hyperinfectious bacteria compared to bacteria from an environmental reservoir. Intestinal passage of *C. rodentium* promotes the expression of T3SS effectors (132, 145) and *eutR* (Fig. 3-5D). Additionally, hyperinfectious bacteria more rapidly adapt to colonize a new host intestinal tract (59). These data support the idea that the population of virulent *C. rodentium* that is shed in stool is critical for transmission and naïve host adaptation (134). In agreement, we demonstrate that EutR promotes virulence gene expression following intestinal passage (Fig. 3-8A-C) and higher levels of fecal shedding following fecal-oral transmission at 2- and 4-days post exposure (Fig. 3-10C-D) compared to infection with an overnight culture via oral gavage (Fig. 3-5A). Therefore, EutR-dependent regulation of *C. rodentium* gene expression contributes to hypertransmissibility and accelerated host adaptation.

An ongoing area of work is to further elucidate the effect of host passage on *C. rodentium* gene expression and the impact of EutR in this process. While a limited number of T3SS virulence factors that contribute to this hyperinfectious phenotype have been identified (145), an unbiased evaluation has not been performed. Analyzing the gene expression of WT grown *in vitro* and WT following host passage will illuminate mechanisms that contribute to this hyperinfectious phenotype, and comparing these data with  $\Delta$ *eutR* gene expression *in vitro* and following host passage will clarify the role of EutR in this process.

Overall, this work reveals a critical strategy by which enteric pathogens alter gene regulation in the intestinal environment to promote maintenance in a host population.

## **Materials and Methods**

### **Strains, plasmids, and recombinant DNA**

All strains and plasmids are listed in Table 3. DBS100 lacks antibiotic resistance; therefore, we used unresolved strains for mouse infections. Bacteria were grown overnight (O/N) shaking in Luria-Bertani (LB) at 37°C. For the growth curve, O/N cultures were diluted 1:100 into M9 minimal medium, which was prepared as previously described without the addition of a nitrogen source (109). EA hydrochloride (10 mM; Sigma) was added as the nitrogen source, and 150 nM AdoCbl (cyanocobalamin; Sigma), a required cofactor for EutR-dependent gene regulation and EA metabolism (67, 79), was also added. Dulbecco's Modified Eagle Medium was purchased from Invitrogen, and EA and AdoCbl were added as indicated.

*C. rodentium* deletion strains were generated using  $\lambda$ -red mutagenesis (112). Briefly, PCR products (using primers listed in Table 4) were amplified from plasmid pKD3 ( $\Delta lacZ$ ) or pKD4 ( $\Delta eutR$ ,  $\Delta eutB$ , and  $\Delta eutC$ ) with flanking regions matching *lacZ*, *eutR*, *eutB*, or *eutC* genes. The PCR products were transformed into *C. rodentium* expressing the Red genes from plasmid pKD46. The deletions were confirmed by sequencing.

The *eutR* mutant was complemented with a plasmid expressing *eutR* under the control of its own promoter. This plasmid was constructed by amplifying *C. rodentium* genomic DNA using primers specific to the *eutR* gene, including 206 nucleotides upstream of the ATG start site (using primers listed in Table 4). Amplified DNA was digested with NheI and SacI and inserted into pGEN-MCS (113) (Addgene MTA). As a control, the wt and  $\Delta eutR$  strains were transformed with the empty pGEN-MCS vector.

### Sequence alignments

EutR, *eutS*, and *ler* sequences were obtained using the annotated EHEC EDL933 (148) and *C. rodentium* (50) genomes. The EMBOSS Needle Pairwise Sequence Alignment tool was used to generate the alignments (149).

### RNA extraction and RT-qPCR

Bacterial cells grown *in vitro* or fecal pellets were resuspended in Trizol (Life Technologies). Colonic tissue was harvested, washed with PBS to remove luminal contents, and then homogenized in Trizol. For all samples, RNA was extracted using a PureLink™ RNA Mini Kit (Invitrogen). RT-qPCR (for *in vitro* and colonic samples) was performed as previously described (150) using a one-step reaction using an ABI 7500-FAST sequence detection system and software (Applied Biosystems). For each 10- $\mu$ l reaction mixture, 5  $\mu$ l 2 $\times$  SYBR master mix (Ambion), 0.05  $\mu$ l Multi-Scribe reverse transcriptase (Invitrogen), and 0.05  $\mu$ l RNase inhibitor (Invitrogen) were added. For stool samples, cDNA was synthesized using SuperScript™ II Reverse Transcriptase (Invitrogen) with random primers prior to qPCR to overcome low RNA yields. Reactions are identical as described for RT-qPCR omitting reverse transcriptase and adjustment for final 10  $\mu$ l volume. Primers were designed using Primer Blast (NCBI) to ensure no cross-reactivity to other genes in the *C. rodentium* chromosome. Amplicon length was approximately 100 bp. Amplification efficiency of each primer pair was verified using standard curves of known DNA concentrations. Melting-curve analysis was used to ensure template specificity by heating products to 95°C for 15 s, followed by cooling to 60°C and heating to 95°C while monitoring fluorescence. After the amplification efficiency and template specificity were determined for each primer pair, relative quantification analysis was used to analyze the samples using the following conditions for cDNA generation and

amplification: 1 cycle at 48°C for 30 min, 1 cycle at 95°C for 10 min, and 40 cycles at 95°C for 15 s and 60°C for 1 min. Two technical replicates of each biological replicate were included for each gene target. Data were normalized to the reference controls *rpoA* (*in vitro* samples) or 16S rRNA specific to *C. rodentium* (stool and tissue samples), and analyzed using the comparative critical threshold ( $C_T$ ) method (151). The expression level of the target genes was compared using the relative quantification method (151).

### Transcriptional fusions

The *C. rodentium* *eutR* or *ler* promoter regions were amplified by PCR using primers listed in Table 4. Resulting PCR products were cloned into the pGEN-luxCDABE vector (113) including 434 and 400 nucleotides upstream of the ATG start site and 31 and 43 nucleotides into the coding sequence, respectively.

### Bioluminescence and *in vivo* imaging system analysis

For measurement of gene expression of *C. rodentium* shed in feces, fecal pellets were weighed and resuspended in 1 ml PBS. 100  $\mu$ l of resuspended fecal pellets were placed in a 96-well plate in duplicate. Luminescence was measured by detection of total counts over a 10 s using a Vector 3 multilabel plate reader with the Wallac 1420 Workstation analysis program. Stool luminescence readings were divided by the total CFU enumerated from feces to report a “luminescence / CFU” readout as a measure of *eutR* or *ler* expression per bacterial CFU.

For *in vivo* bioluminescence on living mice, an IVIS Spectrum (Caliper Lifesciences, Alameda, CA) was used. Luminescence (radiance) was quantified using the software program Living Image (Xenogen). Radiance is reported as photons / sec.

### Purification of EutR under native conditions

The plasmid expressing EutR::MBP was constructed by amplifying the *eutR* gene from *C. rodentium* strain DBS100 using AccuTaq polymerase (Sigma) with primers EutRMBP\_F1 and EutRMBP\_R1 (Table 4) and cloning the resulting PCR product into the NcoI/BamHI cloning sites of vector pMAL-c5X. In order to purify the maltose-binding protein (MBP) and MBP-tagged EutR protein, *Escherichia coli* strain BL-21(DE3) containing MBP or EutR::MBP was grown at 37°C in LB with glucose (0.2% final concentration) and ampicillin (100 µg/ml) to an optical density at 600 nm (OD<sub>600</sub>) of 0.5, at which point IPTG was added to a final concentration of 0.3 mM and allowed to induce overnight at 18°C. Cells were harvested by centrifugation at 4,000 × *g* for 20 min and then resuspended in 25 ml column buffer (20 mM Tris-HCl, 200 mM NaCl, 1 mM EDTA) and lysed by homogenization. The lysed cells were centrifuged, and the lysate was loaded onto a gravity column (Qiagen) with amylose resin. The column was washed with column buffer and then eluted with column buffer containing 10 mM maltose. Fractions containing purified proteins were confirmed by SDS-PAGE and Western analysis, and the protein concentration was determined using a nanodrop.

### ChIP-qPCR

ChIP was performed using the *C. rodentium*  $\Delta$ *eutR* strain transformed with the EutR::MBP or MBP plasmid. Strains were grown in DMEM supplemented with 10 mM EA, 150 nM B<sub>12</sub>, and 2.5 µM IPTG until cells reached an OD<sub>600</sub> of approximately 0.8. Cross-linking and ChIP were performed based on established methods (152). Formaldehyde was added (1% final concentration) for cross-linking, and cells were incubated at RT for 15 min. Reactions were quenched with 0.5 M glycine, then samples were pelleted, resuspended in PBS, and washed. Cells were lysed with 2 mg/ml lysozyme and incubated

at 37°C for 30 min. Subsequently, samples were placed on ice and briefly sonicated. Insoluble cell debris was removed by centrifugation, and supernatants were saved. RNase A was added to the tube and incubated at 37°C for 1 h. 100 units of benzonase nuclease (EMD Millipore) were added to digest DNA into smaller fragments (153). Immunoprecipitation was carried out by incubating samples with amylose beads (NEB) in buffer for 2 h at 4°C with gentle mixing. Beads were pelleted and washed. Then, samples were incubated for 10 min at 65°C in elution buffer with occasional gentle mixing. Samples were centrifuged and supernatants were collected. To reverse the cross-link, samples were boiled for 10 min and DNA was purified using the Qiagen PCR purification kit. For ChIP-quantitative PCR (qPCR) experiments, untreated chromatin was de-cross-linked by boiling for 10 min and purified, for use as the “input” control. The fold enrichment of each promoter represents the value of the immunoprecipitated DNA divided by the input unprecipitated DNA. These values were normalized to the values obtained for each promoter precipitated using MBP empty vector in order to account for non-specific enrichment.

#### Electrophoretic mobility shift assays (EMSAs)

EMSAs were performed as previously described (140) with slight modifications. PCR-amplified DNA probes were generated using 5'-biotinylated primers (Table 4), as previously described. EMSAs were performed by adding increasing amounts of purified EutR protein to end-labeled probe (30 ng) in binding buffer (10mM Tris-HCl (pH 8.0), 1 mM Na-EDTA, 80 mM NaCl, 10 mM  $\beta$ -mercaptoethanol, and 4% glycerol) (154) and incubated for 20 min at 37°C. Immediately before loading the samples, Ficoll solution was added to the reaction mixtures. The samples were electrophoresed for approximately 4-5 h at 175 V on a 6% polyacrylamide gel, transferred to Zeta-Probe membranes, and

visualized using the Chemiluminescent Nucleic Acid Detection Module Kit (Thermo Scientific).

### Animal infections

All experiments were approved by the Institutional Animal Care and Use Committee at the University of Virginia School of Medicine. Female C57BL/6J (6-10-week-old) mice were inoculated by oral gavage of  $1 \times 10^9$  CFU of *C. rodentium*. Mice were monitored daily for weight loss and other signs of distress. At the end of each experiment, mice were euthanized by CO<sub>2</sub> asphyxiation followed by cervical dislocation.

### EA measurements

EA levels were measured as previously described (10) with minor modifications. Colons were harvested, weighed, and homogenized in 1.5 ml ultrapure water. Homogenized tissue was incubated with 150  $\mu$ l 40% sulfosalicylic acid (Sigma) for 15 min and then centrifuged at 11,000  $\times g$  for 15 min at room temperature (RT). Then, 1 ml of the supernatant was mixed with 300  $\mu$ l of 0.5 M NaHCO<sub>3</sub> (Sigma), 2 ml of 20 mg/ml dansyl chloride solution (Sigma) in acetone, and 200  $\mu$ l 1M NaOH (Fisher). Following incubation in the dark for 20 min at RT, 200  $\mu$ l of 25% NH<sub>4</sub>OH (Sigma) was added. The volume was adjusted to 5 ml with acetonitrile (Sigma), and 1 ml was centrifuged at 11,000  $\times g$  for 1 min. The supernatant was taken for analysis. The LC-MS system consists of a ThermoElectron Orbitrap ID-X mass spectrometer with a HESI source interfaced to a Thermo Accucore Vanquish C181.5  $\mu$ m, 2.1  $\times$  100mm column. 2  $\mu$ L of the extract was injected and the compounds eluted from the column by a methanol/0.1% formic acid gradient at a flowrate of 250  $\mu$ L/min (15 minutes total time). The nanospray ion source was operated at 3.2 kV. The sample was analyzed by MS and MS/MS. The dansyl-EA

was detected as a peak at ~4.36 min and a mass of 295.111+. A 1 M *in vitro* sample of EA hydrochloride (Sigma) taken through the dansylation process was used to generate a standard curve.

#### CFU enumeration from stool and the colon

For CFU enumerated from stool, fresh fecal pellets were collected at indicated time points, weighed, and homogenized in 1 ml PBS. Serial dilutions were plated on LB plates containing appropriate antibiotic selectivity to evaluate CFU. Enumerated CFU / g stool was log-transformed prior to statistical analysis, as previously described (155). For CFU enumerated from the colon, tissue was flushed with PBS and homogenized. Homogenates were resuspended in PBS, serially diluted, and plated on LB with antibiotics.

#### Transmission studies

Donor mice were infected with WT or  $\Delta$ *eutR* *C. rodentium* for 6 or 10 days. At these timepoints, fecal pellets were collected from the donor mice to measure bacterial burden in stool and *ler* expression (luminescence) as described above. Each donor mouse was placed in a fresh cage with 3 recipient mice for 24 h. At 24 post-cohousing, exposed mice were separated from index mice placed in a fresh cage together for 2 days post exposure (Fig. 3-10C) or placed in individual cages up to 4 days post exposure (Fig. 3-10B and D). At 2 or 4 days following individual caging, stool was collected from each recipient mouse, homogenized in PBS, and plated on appropriate selective media to determine CFU of transmitted *C. rodentium*.

### Immunohistochemistry

Mice were infected with WT *C. rodentium* and euthanized as described above. Colon tissue was harvested, luminal contents were removed, and the tissue was flushed with modified Bouin's fixative. The tissue was placed in cassettes and fixed for 24-48 hours in neutral-buffered formalin (4% formaldehyde). Cassettes were transferred to 70% ethanol, and, in collaboration with the UVA Histology Core, samples were placed on a tissue dehydrator for dehydration and paraffin embedding. Following embedding into a paraffin block, paraffin sections were cut at 5 µm on a Leica microtome. Sections incubated with 1:1600 polyclonal rabbit antibody against the *E. coli*/*C. rodentium* O antigen (Novus Biologicals) and counter-stained with hematoxylin to visualize intestinal tissue. *C. rodentium* was detected using the DISCOVERY OmniMap Anti-Rb HRP detection system and DISCOVERY ChromoMap DAB Kit (Ventana Co.).

### Statistical analyses

Statistical analyses were performed using GraphPad Prism software version 8.0 (GraphPad Software Inc.). Group comparisons were performed using Student's t-test for *in vitro* analyses and the Wilcoxon signed-rank test for all *in vivo* analyses.

## Figures

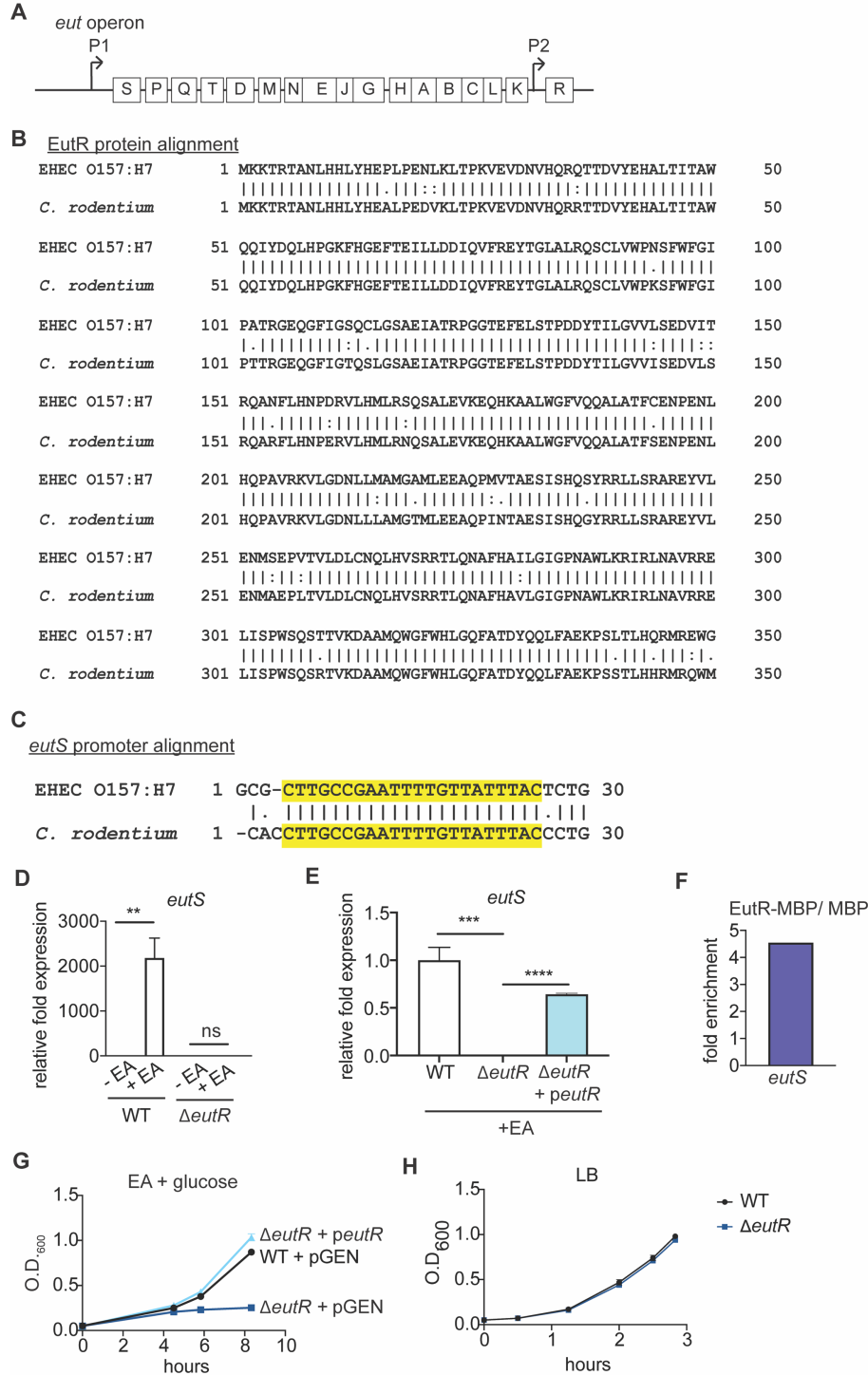


**Fig. 3-1. *C. rodentium* EutR binds to the conserved *eutS* promoter to support *eut* gene expression and growth using EA. (A) Schematic of the *eut* operon in *C. rodentium*.**

(B) Alignment of EutR amino acid sequences from EHEC and *C. rodentium*. (C) Alignment of *eutS* promoter regions from EHEC and *C. rodentium*, with the conserved EutR binding region highlighted in yellow. For (B) and (C) alignments generated using EMBOSS Needle, “|” indicates a conserved residue, “:” indicates a similarity score > 1.0, and “.” indicates a small positive alignment score. (D) RT-qPCR of *eutS* expression in WT and  $\Delta$ *eutR* *C. rodentium* strains grown in the absence or presence of EA. n=3. (E) RT-qPCR of *eutS* expression in WT,  $\Delta$ *eutR*, and complemented *C. rodentium* strains grown in the presence of EA. (F) qPCR showing enrichment of *eutS* from *in vivo* ChIP of EutR::MBP compared to MBP. n=2. (G) Growth curve showing WT,  $\Delta$ *eutR*, and complemented *C. rodentium* strains grown in a M9 minimal medium containing EA. (H) Growth curve showing WT and  $\Delta$ *eutR* in LB. Error bars represent the mean +/- standard deviation (SD). \*\* , p < 0.01; \*\*\* p < 0.001; \*\*\*\* , p < 0.0001.

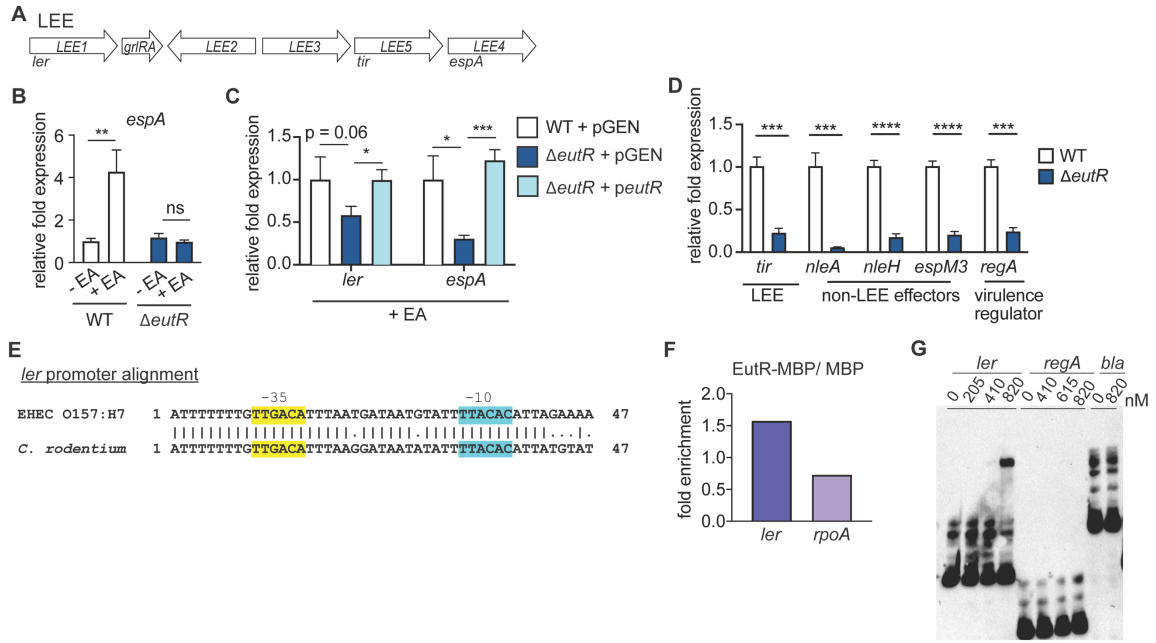


**Fig. 3-2. *C. rodentium* EutR directly regulates *ler* and promotes virulence gene expression.** (A) Schematic of the LEE. (B) RT-qPCR of *espA* gene expression from strains grown in the presence or absence of EA. n = 3. (C) RT-qPCR of *ler* and *espA* gene expression in WT,  $\Delta eutR$ , and complemented *C. rodentium* strains grown in the presence of EA. n = 3. (D) RT-qPCR of indicated virulence genes from strains grown in the presence of EA. n = 3. (E) Alignment of EHEC and *C. rodentium* *ler* promoter regions. (F) qPCR showing enrichment of *ler* and *rpoA* from *in vivo* ChIP of EutR::MBP compared to MBP. n=2. (G) EMSA of *ler*, *regA*, and *bla* promoter probes with EutR::MBP with increasing nM concentrations of EutR::MBP. Error bars represent the mean +/- SD. \*,  $p < 0.05$ ; \*\*,  $p < 0.01$ ; \*\*\*,  $p < 0.001$ ; \*\*\*\*,  $p < 0.0001$ .

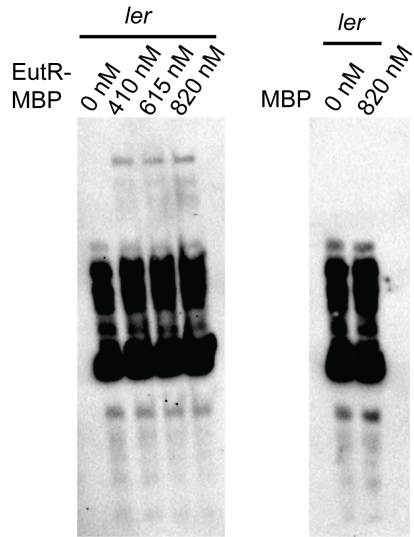


**Fig. 3-3. EutR directly binds the *ler* promoter.** EMSA of *ler* promoter probe with EutR-MBP or MBP alone.

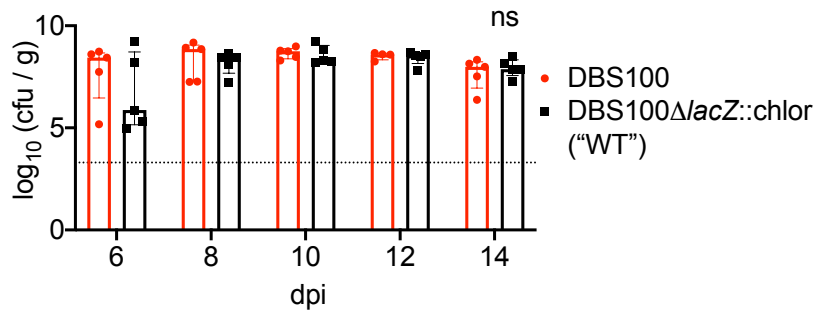


**Fig. 3-4. DBS100 and DBS100ΔlacZ::chlor (used as “WT”) strains enumerated from stool during infection.** Median +/- interquartile range (IQR) shown. The dashed line represents the limit of detection (LOD).

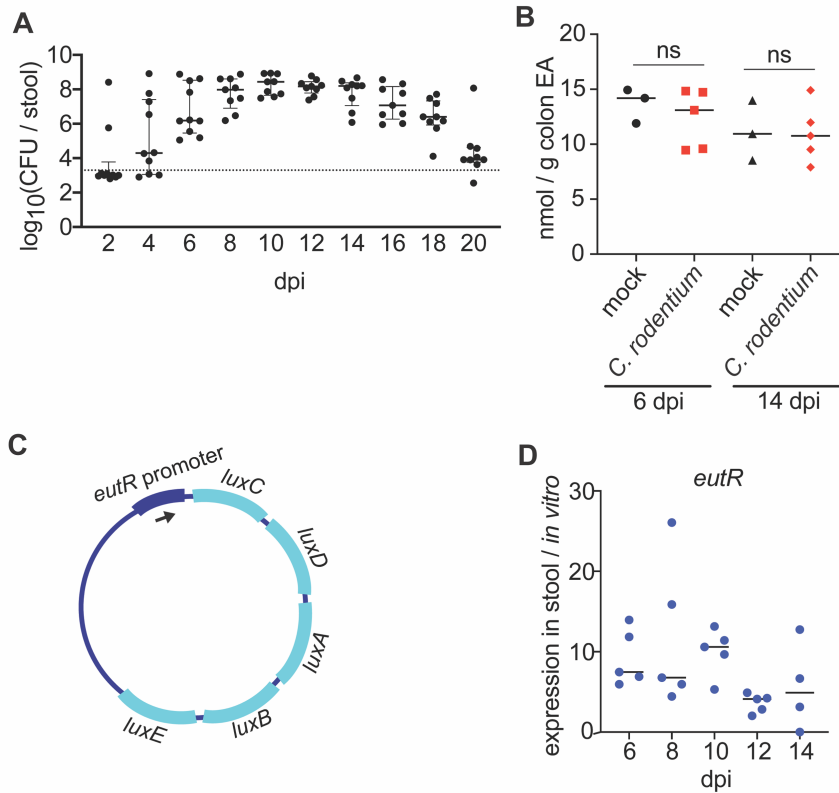


**Fig. 3-5. *C. rodentium* shedding in stool, EA levels, and *eutR* expression during infection.** (A) Enumeration of WT *C. rodentium* shed in stool over the course of infection. Data presented as median +/- IQR. (B) EA levels measured from colon tissue containing luminal contents from mock-infected or WT *C. rodentium*-infected mice. (C) Schematic of the *eutR* promoter fused to the pGEN-luxCDABE luminescent reporter system. (D) *eutR* expression in *C. rodentium* shed in stool compared to *eutR* grown *in vitro*. Data are normalized to CFU. The dashed line in A represents the LOD.

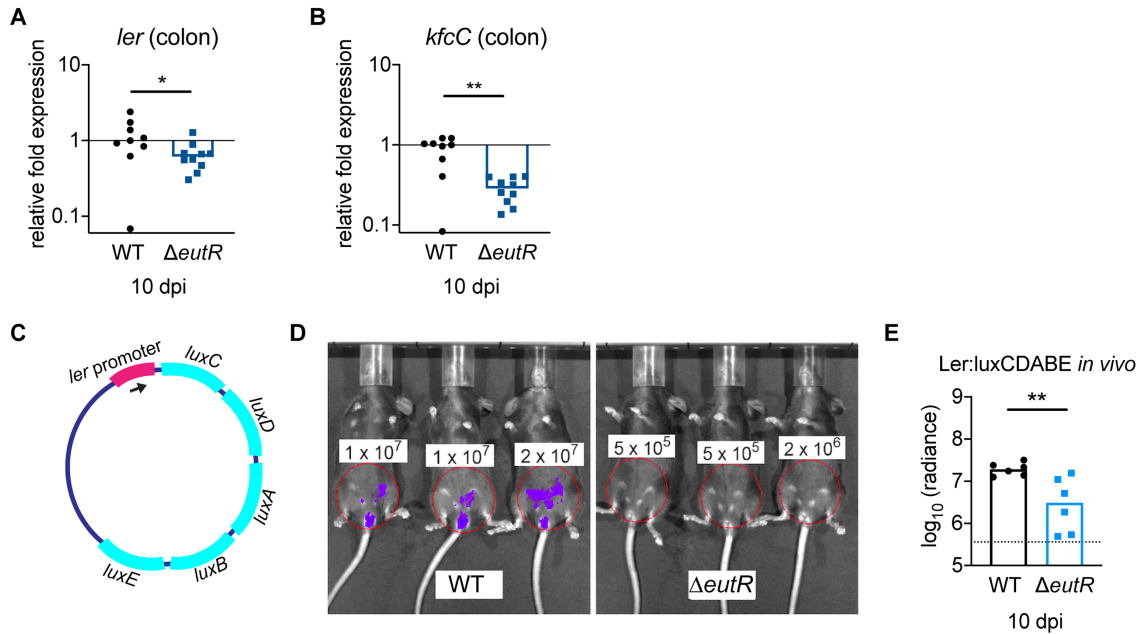


**Fig. 3-6. EutR enhances virulence gene expression *in vivo*.** (A) RT-qPCR of *ler* expression of WT and  $\Delta eutR$  in the colon with luminal contents removed. (B) RT-qPCR of *kfcC* expression of WT and  $\Delta eutR$  in the colon with luminal contents removed. (C) Schematic of the *ler* promoter fused to the pGEN-luxCDABE fluorescent reporter system. (D) Representative images of *C. rodentium ler* expression at 10 dpi and (E) quantified *ler* expression at 10 dpi. Radiance is measured as photons / second. The dashed lines in (E) represent the background expression measured in mock-infected animals. \*,  $p < 0.05$ ; \*\*,  $p < 0.01$ .

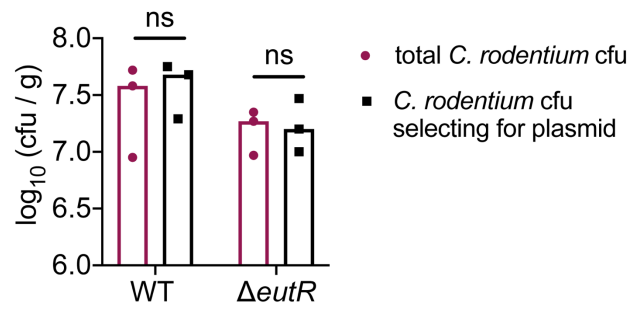


**Fig. 3-7. *Ler::luxCDABE* is retained in *C. rodentium* shed in stool.** *C. rodentium* enumerated from stool at 10 dpi plated on media selective for *C. rodentium* or on media selective for *C. rodentium* containing the pGEN-*luxCDABE* plasmid with the *ler* promoter.

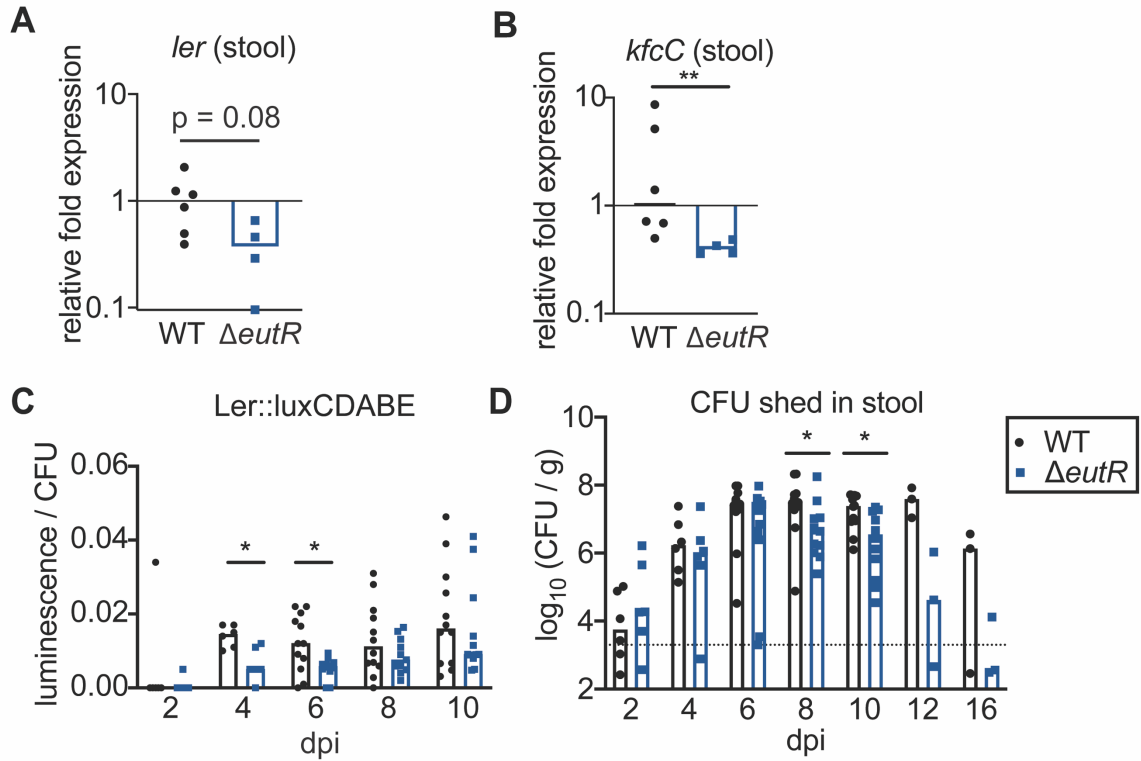


**Fig. 3-8. EutR promotes the virulence gene expression and bacterial burden of *C. rodentium* shed in stool.** (A) RT-qPCR of *ler* gene expression of *C. rodentium* shed in stool at 10 dpi. (B) RT-qPCR of *kfcC* fimbriae expression by *C. rodentium* associated with colon tissue. (C) *ler* expression per *C. rodentium* CFU over time. (D) Enumeration of *C. rodentium* CFU. The dashed line represents the LOD. \*,  $p < 0.05$ ; \*\*,  $p < 0.01$ .

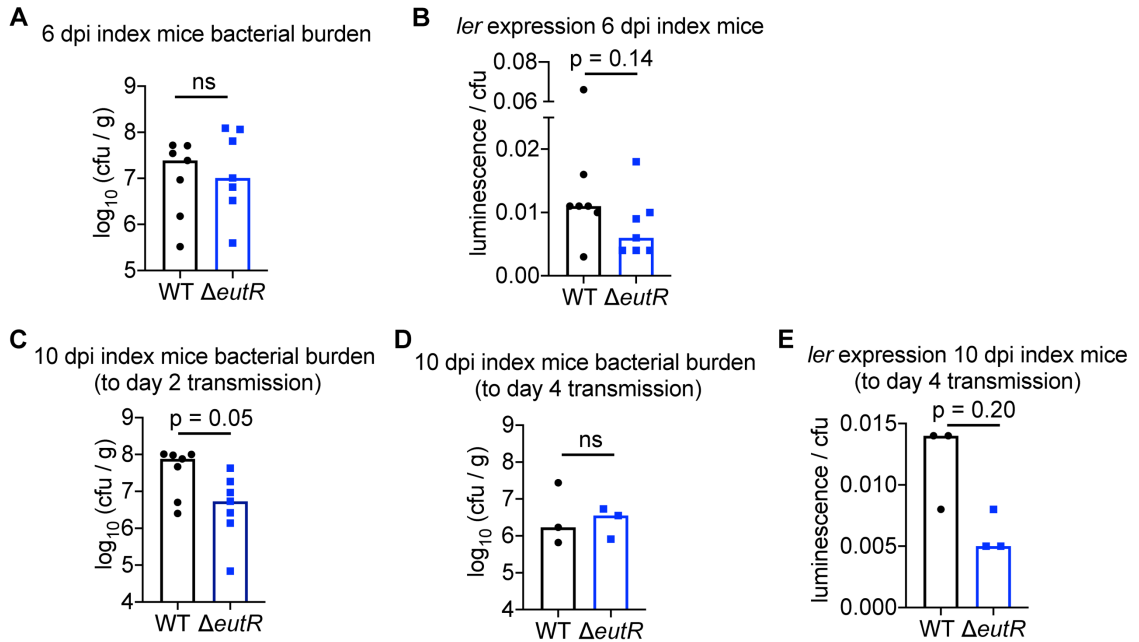


**Fig. 3-9. *ler* expression and *C. rodentium* burden shed in stool of index mice used for transmission experiments.** (A) Enumeration of the stool CFU of 6 dpi index mice, corresponding to Fig. 3-10B. (B) *ler* expression measured by luminescence per CFU of 6 dpi index mice, corresponding to Fig. 3-10B. (C) Enumeration of the stool CFU of 10 dpi index mice, corresponding to Fig. 3-10C. (D) Enumeration of the stool CFU of 10 dpi index mice, corresponding to Fig. 3-10D. (E) *ler* expression measured by luminescence per CFU of 10 dpi index mice, corresponding to Fig. 3-10D.

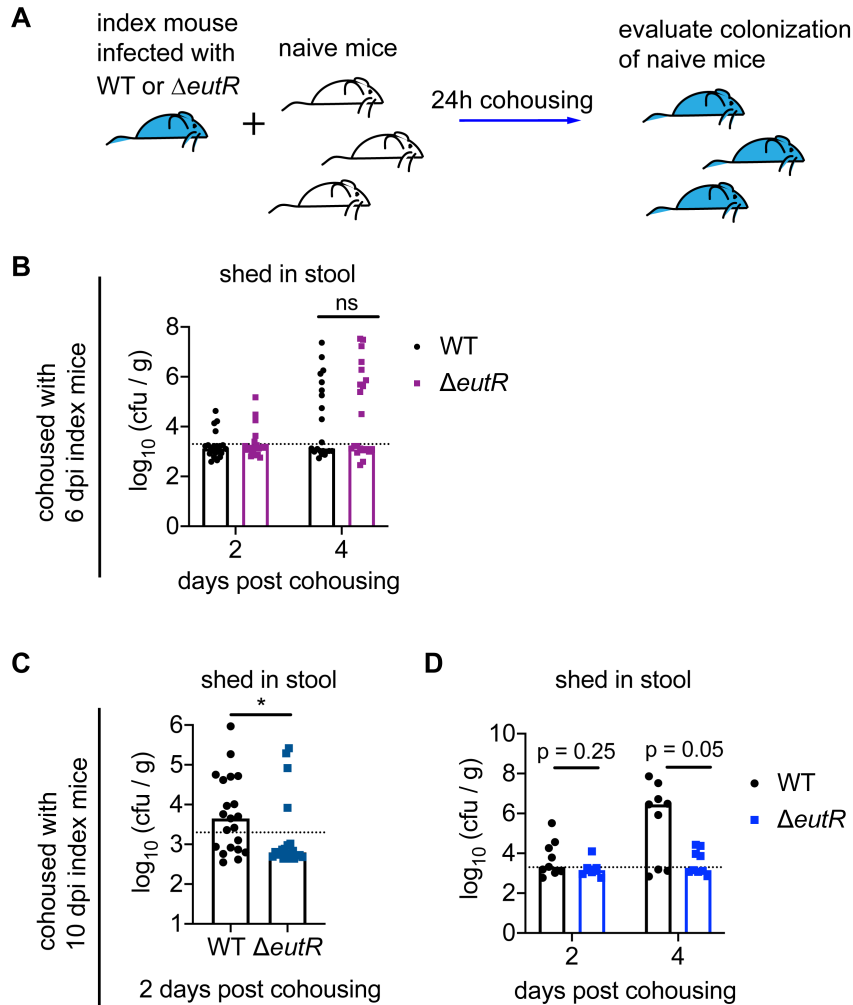


**Fig. 3-10. EutR promotes *C. rodentium* transmission to naïve hosts.** (A) Schematic of the experimental setup of cohousing transmission experiments. (B) Enumeration of *C. rodentium* shed in stool from naïve mice following cohousing with 6 dpi index mice. (C) Enumeration of *C. rodentium* shed in stool at 2 dpi from naïve mice following cohousing with 10 dpi index mice. (D) Enumeration of *C. rodentium* shed in stool at 2 and 4 dpi from naïve mice following cohousing with 10 dpi index mice.

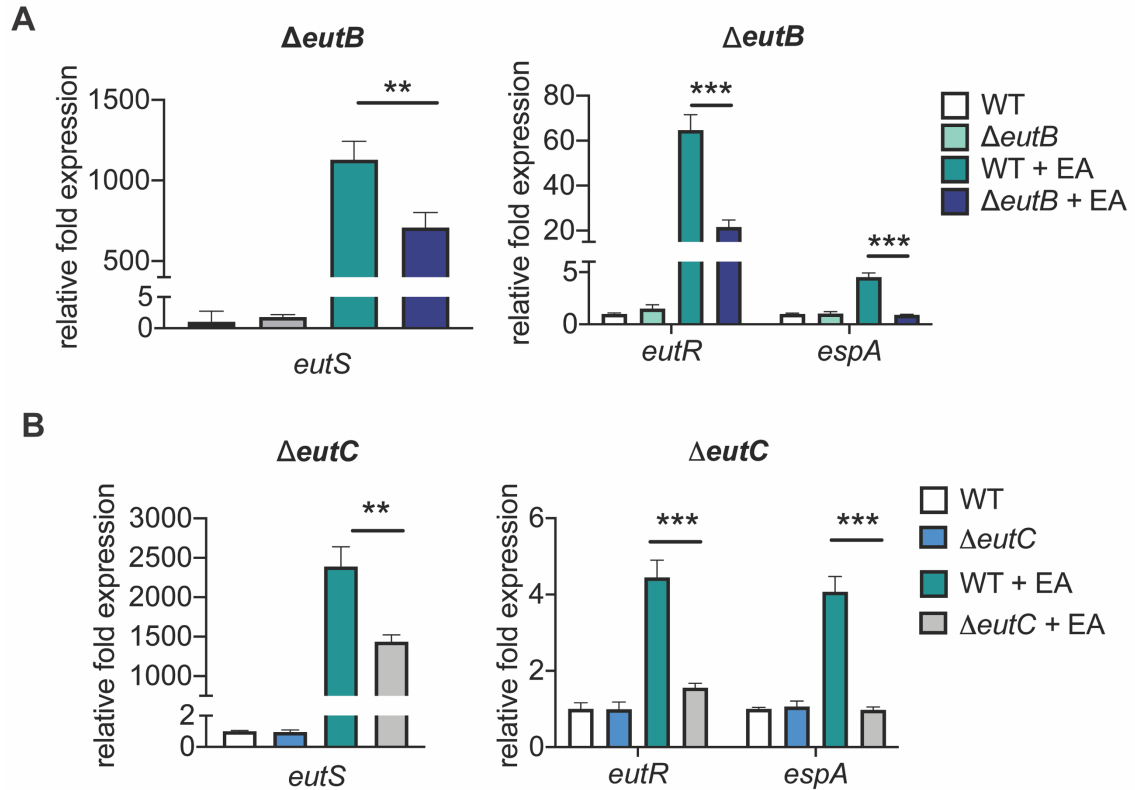


**Fig. 3-11. Gene expression in *C. rodentium* *eut* metabolic mutants.** (A) RT-qPCR of *eutS*, *eutR*, and *espA* gene expression from WT and  $\Delta$ *eutB* strains grown in the absence or presence of EA. n = 3. (B) RT-qPCR of *eutS*, *eutR*, and *espA* gene expression from WT and  $\Delta$ *eutC* strains grown in the absence or presence of EA. n = 3. Error bars represent the mean  $\pm$  SD. \*\* p < 0.01, \*\*\* p < 0.001.

colon tissue colonization

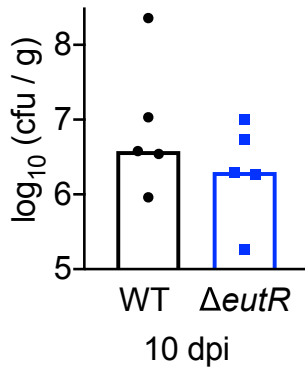


**Fig. 3-12. The effect of EutR on *C. rodentium* colonization in the colon.** Enumeration of *C. rodentium* in the colon without luminal contents at 10 dpi.

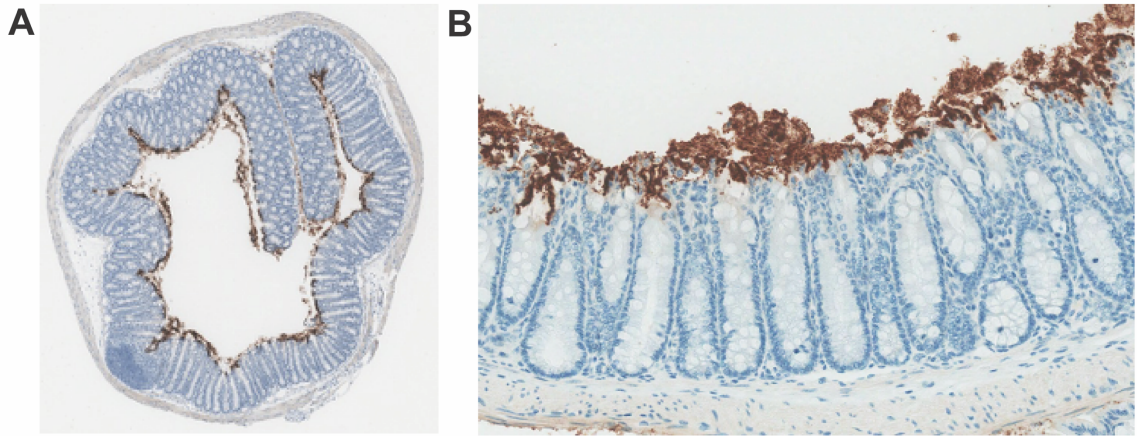


**Fig. 3-13. Immunohistochemical staining of *C. rodentium* at the colonic epithelium.**

(A) A colonic tissue section from a mouse infected with WT *C. rodentium* at 120x magnification. (B) A colonic tissue section from a mouse infected with WT *C. rodentium* at 480x magnification.

## **Chapter 4: Summary and Implications to the Field**

## Summary

Intestinal bacteria have evolved to sense the metabolite EA to alter gene expression and promote metabolism. Enterobacteriaceae encode a conserved *eut* operon to metabolize EA (70). The field generally views EA metabolism as an ability that confers pathogens with an intestinal growth advantage over the microbiota. This thought became prevalent following a study that examined EA metabolism by commensal *E. coli* and reported minimal *eut* gene expression in response to EA (84). However, *eut* genes are highly conserved among members of the intestinal microbiota, including commensal *E. coli* (63). Therefore, we re-evaluated EA metabolism by human commensal *E. coli* and directly compared growth between EHEC and commensal *E. coli* using EA. In challenge to the previous study, we determined that two human commensal *E. coli* strains respond to EA to alter *eut* gene expression and support growth using EA. Furthermore, in co-culture, commensal *E. coli* outgrew EHEC using EA. These data demonstrate that human commensal *E. coli* not only metabolize EA but outgrow a pathogen in direct competition. In addition to EA metabolism, pathogenic Enterobacteriaceae sense EA to regulate metabolism-independent gene expression. In our studies, we demonstrate that commensal *E. coli* also respond to EA to alter the expression of fimbrial genes. Overall, these data show a role for EA in commensal *E. coli* growth and gene expression.

In EHEC, EutR senses EA to directly regulate virulence gene expression (81, 88), which promotes EHEC pathogenesis. The master virulence regulator Ler enhances the expression of genes encoded by the LEE pathogenicity island, which encodes proteins that form a T3SS and AE lesions on host epithelial cells (81, 88, 91). The role of EutR in EHEC pathogenesis in the intestinal environment has not been investigated; therefore, we used the *C. rodentium* mouse model of EHEC infection to examine the impact of EutR *in vivo*. We determined that EutR-dependent regulation of *eut* gene expression and virulence

gene regulation are conserved in *C. rodentium*. Furthermore, *eutR* expression is upregulated in *C. rodentium* following intestinal passage throughout infection. EutR also promotes *C. rodentium* virulence gene expression *in vivo*, the bacterial burden shed in stool, and effective transmission to naïve hosts. These studies demonstrate the central role of EutR during intestinal infection, impacting multiple stages of pathogenesis. Through these two projects, we have gained insight into the shared and divergent uses of a conserved nutrient sensing pathway among commensal and pathogenic intestinal bacteria (Fig. 4-1).

### **Implications to the Field**

Through this work, we have challenged the dogma that EA is a noncompetitive metabolite used by pathogens for growth but not the microbiota. In contrast, our data suggest that human commensals not only grow using EA but replicate faster than EHEC using EA (Fig. 2-4A-D). These findings have implications for how we understand EA utilization in the intestinal tract and challenge the idea that these pathways should be generally associated with virulence and targeted for therapeutic intervention. In addition to commensal *E. coli*, abundant members of the microbiota (63), such as nonpathogenic strains of *Clostridia* (156, 157) and *Enterococcus* (83, 99), encode *eut* loci and may metabolize high levels of EA in the intestinal tract. EA concentrations may be limiting in local microenvironments where the microbiota and a pathogen compete for EA. Therefore, the microbiota may provide nutritional resistance against pathogens, even pathogens that also utilize EA. Alternatively, sufficient EA concentrations may be present for both members of the microbiota and pathogens to consume. Further studies are warranted to explore the balance in EA utilization among the microbiota and pathogens.

Furthermore, our studies expand the model of EA-dependent gene expression in the intestinal tract. EA has driven the conservation of *eut* genes among diverse bacteria, which promote EA metabolism (68). Pathogens also sense EA to regulate the expression of genes unrelated to EA metabolism (81, 88, 91, 140). Not only have we shown that commensal *E. coli* sense EA to express *eut* genes and to metabolize EA, our studies demonstrate a role for EA-dependent signaling in commensal *E. coli*; EA alters fimbrial gene expression in commensal *E. coli*, which may affect intestinal colonization. While metabolites have been shown to act as effector ligands to affect gene expression in commensal bacteria (11, 12), more work has been devoted to understanding how pathogens use host metabolites to promote virulence (6). Improved understanding of mechanisms by which the microbiota has adapted to long-term occupation of a host niche is important to support a healthy intestinal environment.

Additionally, we link sensing of an intestinal metabolite to pathogen virulence, colonization, and transmission to naïve hosts. Until this study, the effect of EutR on intestinal virulence gene expression was unexplored. We show that EutR affects *in vivo* expression of a central virulence regulator and a fimbrial gene (Fig. 3-6, 3-8A-C), which impact host colonization (48, 126). Despite the critical role of transmission to the propagation of an enteric pathogen in a host population, transmission is a woefully understudied area. Previous work has demonstrated that virulence gene deletion has a negative effect on *C. rodentium* transmission (123) and that a certain colonization burden is important for effective transmission (59). However, this is the first study to connect a conserved regulatory pathway with gene expression, colonization, and transmission. Effective transmission allows for the propagation of a pathogen in a host population; these studies challenge the field to further investigate mechanisms by which transmission is regulated.

Together, this work reveals a conserved mechanism of metabolite sensing that impacts commensal and pathogenic Enterobacteriaceae.

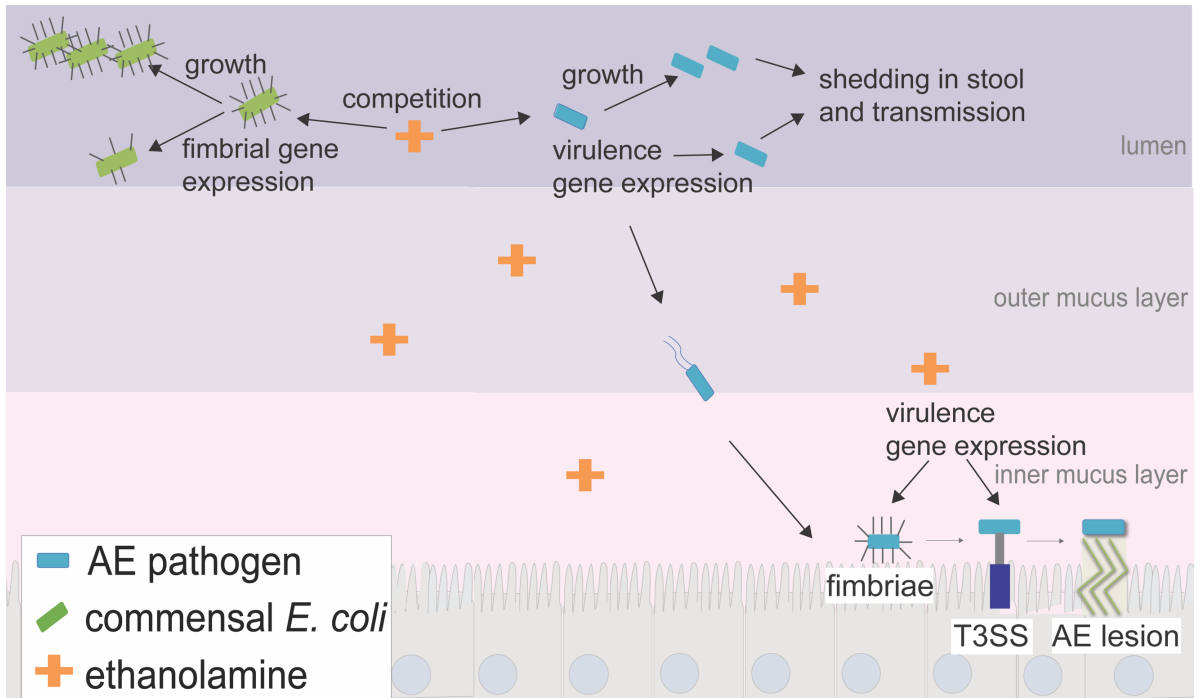


**Fig. 4-1. Summary of the work described in Chapters 2 and 3.**

EA utilization by commensal *E. coli* and AE pathogens in the colon.

## Appendix

Table 1. Bacterial strains used in Chapter 2

<b>Strain</b>	<b>Genotype description</b>	<b>Reference or source</b>
HS	<i>E. coli</i> human commensal strain	(20)
MK85	<i>E. coli</i> HS <i>eutR</i> deletion strain	This study
Nissle 1917	<i>E. coli</i> human commensal strain	(22, 23)
86-24	Wild-type EHEC (serotype O157:H7)	(158)
<b>Plasmid</b>		
pGEN	Cloning vector	(113)
pCAR01	pGEN + <i>E. coli</i> HS <i>eutR</i>	This study

Table 2. Oligonucleotides used in Chapter 2

Primer name	Sequence	Primer use
HS_LR_eutR_F1	CCCGGCATTAACATCATGAAAAAGACC CGTACAGCCAATTTGCACCATCTTTGT GTAGGCTGGAGCTGCTTC	$\lambda$ -Red
HS_LR_eutR_R1	AAGTGAGTTTATTAAGGTCAGGGATTG GGTGTAACCTCCCTCACCCCACTCTCA TATGAATATCCTCCTTAG	$\lambda$ -Red
pGEN_HS_eutR_F	CTAGGAGCTCTGTTGGCGCTGTTAACA TCA	<i>E. coli</i> HS <i>eutR</i> complement
pGEN_HS_eutR_R	CTAGGCTAGCTCACCCCACTCCCGCA TCC	<i>E. coli</i> HS <i>eutR</i> complement
HS_rpoA_F	CGCGGTCGTGGTTATGTG	RT-qPCR
HS_rpoA_R	GCGCTCATCTTCTTCCGAAT	RT-qPCR
HS_eutS_F	GGCGGCGACTCATGGATAAA	RT-qPCR
HS_eutS_R	TTCTTCGCCAGTTCCTCACC	RT-qPCR
HS_eutB_F	GCGTGCGGGCAAAGC	RT-qPCR
HS_eutB_R	CACCGGATTATTGCGGATGT	RT-qPCR
HS_eutR_F	ATCCGGGCAAGTTTCATGGT	RT-qPCR
HS_eutR_R	CGGAATGCCAAACCAGAACG	RT-qPCR
Nissle_rpoA_F	CGCGGTCGTGGTTATGTG	RT-qPCR
Nissle_rpoA_R	GCGCTCATCTTCTTCCGAAT	RT-qPCR
Nissle_eutS_F	CCGGATGCGGGCGCAATCGG	RT-qPCR
Nissle_eutS_R	CGATATGCACATCGGCGGCT	RT-qPCR
Nissle_eutB_F	GCGTGCGGGCAAAGC	RT-qPCR
Nissle_eutB_R	CACCGGATTATTGCGGATGT	RT-qPCR
Nissle_eutR_F	ATCCGGGCAAGTTTCATGGT	RT-qPCR
Nissle_eutR_R	CGGAATGCCAAACCAGAACG	RT-qPCR
HS_yad_RT_F1	AGGTTTTGCCCTGTCTGGTC	RT-qPCR
HS_yad_RT_R1	TGCAGCAGGATCAGACCATC	RT-qPCR
HS_ybg_RT_F1	AGATATCGACCTGGCTCCGA	RT-qPCR
HS_ybg_RT_R1	GGTTGCATTGCGCGTAACTG	RT-qPCR

Table 3. Bacterial strains used in Chapter 3

	<b>Genotype description</b>	<b>Reference or source</b>
<b>Strains</b>		
DBS100	<i>Citrobacter rodentium</i>	Schauer 1993 Infect. Immun.; received as a gift from James Nataro
DBS100 $\Delta$ <i>lacZ</i> ::chlor	unresolved <i>lacZ</i> deletion strain, used as "WT" in this study	This study
DBS100 $\Delta$ <i>eutR</i> ::kan	unresolved <i>eutR</i> deletion strain	This study
<b>Plasmids</b>		
pGEN	Cloning/expression vector	pGEN-MCS was a gift from Harry Mobley (Addgene plasmid # 44919)
pGEN:: <i>eutR</i>	<i>C. rodentium eutR</i> plus 206 bp upstream region in pGEN	This study
pGEN-luxCBADE	Cloning/expression vector	pGEN-luxCDABE was a gift from Harry Mobley (Addgene plasmid # 44918)
pGEN-luxCBADE:: <i>eutR</i> prom	434 bp upstream and 31 bp into <i>eutR</i> coding region in pGEN-luxCDABE	This study
pGEN-luxCBADE:: <i>ler</i> prom	400 bp upstream and 43 bp into <i>ler</i> coding region in pGEN-luxCDABE	This study

Table 4. Oligonucleotides used in Chapter 3

Primer name	Sequence	Primer use
CR_LR_lacZ_F1	TGCTCGTATGTTGTTTTAAATTGTGAGCGGATAAC AATTTTTAACAGGTGTGTAGGCTGGAGCTGCTTC	Lambda red recombination to generate <i>C. rodentium lacZ</i> deletion strain
CR_LR_lacZ_R1	GGTTTTTATTATTTCTGGCCCCAGACGATCTGGTA GTGGTAGCGTCCTGCATATGAATATCCTCCTTAG	Lambda red recombination to generate <i>C. rodentium lacZ</i> deletion strain
CR_LR_eutR_F1	ATCATGAAAAAGACCCGTACAGCCAATTTGCACC ATCTTTATCATGAAGCATGTGTAGGCTGGAGCTG CTTC	Lambda red recombination to generate <i>C. rodentium eutR</i> deletion strain
CR_LR_eutR_R1	GTATTTTCTCACATCCACTGGCGCATTTCGGTGAT GCAGCGTCGATGACGGCTCATATGAATATCCTCC TTAG	Lambda red recombination to generate <i>C. rodentium eutR</i> deletion strain
CR_LR_eutB_F1	CTTatgAAACTAAAGACCACATTGTTTCGGCAATGTT TATCAGTTTAAGGATGTGTGTAGGCTGGAGCTGC TTC	Lambda red recombination to generate <i>C. rodentium eutB</i> deletion strain
CR_LR_eutB_R1	CCGCGTCATCAGAAGAACAGAGACGGATCGCCC GCCCGTTTGGTCAAACGACCATATGAATATCCTC CTTAG	Lambda red recombination to generate <i>C. rodentium eutB</i> deletion strain
CR_LR_eutC_F1	TTTGACCAAACGGGCGGGCGATCCGTCTCTGTTC TTCTGATGACGCGGGTGTAGGCTGGAGCTGCTTC	Lambda red recombination to generate <i>C. rodentium eutC</i> deletion strain
CR_LR_eutC_R1	ATGCCTCCTTAACGGGTCATGTTGATGCCGGATG CTTTCTGCTCCAGCACATATGAATATCCTCCTTAG	Lambda red recombination to generate <i>C. rodentium eutC</i> deletion strain
pGEN_CR_eutR_F	CTAGGAGCTCCTGTTGGCAAAGCTCGGCGA	Cloning <i>C. rodentium eutR</i> plus 206 bp upstream to

		insert into pGEN
pGEN_CR_eutR_R	CTAGGCTAGCTCACATCCACTGGCGCATTC	Cloning <i>C. rodentium</i> <i>eutR</i> plus 206 bp upstream to insert into pGEN
EutRMBP_F1	ATCCATGGGCATGAAAAAGACCCGTACA	Cloning <i>C. rodentium</i> <i>eutR</i> into pMAL
EutRMBP_R1	ATGGATCCTCACATCCACTGGCGCAT	Cloning <i>C. rodentium</i> <i>eutR</i> into pMAL
EMSA_ierprom_F1	GGCGAGCCGCTTACTCTAAA	5' biotinylated, for EMSA
EMSA_ierprom_R1	ACCCCTATAAAAGCTATTAACCCCT	5' biotinylated, for EMSA
EMSA_regAprom_F1	TACAGAGGTAAGGGATAACTCATTG	5' biotinylated, for EMSA
EMSA_regAprom_R1	TGGGTTATCAGCTATGTAACTCG	5' biotinylated, for EMSA
EMSA_blaprom_F1	GGAATTCGAAAGGGCCTCGTG	5' biotinylated, for EMSA
EMSA_blaprom_R1	CGGGATCCGGTGAGCAAAAAC	5' biotinylated, for EMSA
ierprom_RT_F	GGCGAGCCGCTTACTCTAAA	ChIP-qPCR
ierprom_RT_R	ACCCCTATAAAAGCTATTAACCCCT	ChIP-qPCR
eutSprom_RT_F	GGTTCTCCCGCGCATTAAATAAT	ChIP-qPCR
eutSprom_RT_R	CGCCAGCGTGACCTGTTTA	ChIP-qPCR
CR_rpoA_F	AATCGCCTCTTCAGGATCGA	ChIP-qPCR, RT-qPCR
CR_rpoA_R	CGTACCGACCTGGACAAGCT	ChIP-qPCR, RT-qPCR
CR_eutS_F	CAGGAATTTGTGCCGGGTAA	RT-qPCR

## References

1. N. Kamada, G. Y. Chen, N. Inohara, G. Nunez, Control of pathogens and pathobionts by the gut microbiota. *Nat Immunol* **14**, 685-690 (2013).
2. R. Maltby, M. P. Leatham-Jensen, T. Gibson, P. S. Cohen, T. Conway, Nutritional basis for colonization resistance by human commensal *Escherichia coli* strains HS and Nissle 1917 against *E. coli* O157:H7 in the mouse intestine. *PLoS One* **8**, e53957 (2013).
3. M. T. Sorbara, E. G. Pamer, Interbacterial mechanisms of colonization resistance and the strategies pathogens use to overcome them. *Mucosal Immunology* **12**, 1-9 (2018).
4. G. den Besten *et al.*, The role of short-chain fatty acids in the interplay between diet, gut microbiota, and host energy metabolism. *J Lipid Res* **54**, 2325-2340 (2013).
5. J. K. Nicholson *et al.*, Host-gut microbiota metabolic interactions. *Science* **336**, 1262-1267 (2012).
6. B. C. Lustrì, V. Sperandio, C. G. Moreira, Bacterial Chat: Intestinal Metabolites and Signals in Host-Microbiota-Pathogen Interactions. *Infect Immun* **85**, (2017).
7. J. K. Nicholson, I. D. Wilson, in *Nat Rev Drug Discov.* (England, 2003), vol. 2, pp. 668-676.
8. M. Rajilic-Stojanovic, W. M. de Vos, The first 1000 cultured species of the human gastrointestinal microbiota. *FEMS Microbiol Rev* **38**, 996-1047 (2014).
9. P. H. Degnan, N. A. Barry, K. C. Mok, M. E. Taga, A. L. Goodman, Human gut microbes use multiple transporters to distinguish vitamin B(1)(2) analogs and compete in the gut. *Cell Host Microbe* **15**, 47-57 (2014).
10. P. Thiennimitr *et al.*, Intestinal inflammation allows *Salmonella* to use ethanolamine to compete with the microbiota. *Proc. Natl. Acad. Sci.* **108**, 17480-17485 (2011).
11. M. Lempp *et al.*, Systematic identification of metabolites controlling gene expression in *E. coli*. *Nature Communications* **10**, 1-9 (2019).
12. B.-K. Cho, S. Federowicz, Y.-S. Park, K. Zengler, B. Ø. Palsson, Deciphering the transcriptional regulatory logic of amino acid metabolism. *Nature Chemical Biology* **8**, 65-71 (2011).
13. A. R. Pacheco *et al.*, Fucose Sensing Regulates Bacterial Intestinal Colonization. *Nature* **492**, 113-117 (2012).
14. A. Kumar, V. Sperandio, A. Casadevall, Indole Signaling at the Host-Microbiota-Pathogen Interface. (2019).
15. S. Octavia, R. Lan, in *The Prokaryotes*. (SpringerLink, 2014), pp. 225-286.
16. J. T. Poolman, M. Wacker, in *J Infect Dis.* (2016), vol. 213, pp. 6-13.
17. P. B. Eckburg *et al.*, Diversity of the human intestinal microbial flora. *Science* **308**, 1635-1638 (2005).
18. H. Z. Apperloo-Renkema, B. D. Van der Waaij, D. Van der Waaij, Determination of colonization resistance of the digestive tract by biotyping of Enterobacteriaceae. *Epidemiol Infect* **105**, 355-361 (1990).
19. M. M. Levine *et al.*, Diarrhea caused by *Escherichia coli* that produce only heat-stable enterotoxin. *Infect Immun* **17**, 78-82 (1977).
20. M. M. Levine *et al.*, *Escherichia coli* strains that cause diarrhoea but do not produce heat-labile or heat-stable enterotoxins and are non-invasive. *Lancet* **1**, 1119-1122 (1978).

21. D. A. Rasko *et al.*, The pangenome structure of *Escherichia coli*: comparative genomic analysis of *E. coli* commensal and pathogenic isolates. *J Bacteriol* **190**, 6881-6893 (2008).
22. N. A. (Deutsche Medizinische Wochenschrift, 1925), vol. 44, pp. 1809–1813.
23. U. Sonnenborn, *Escherichia coli* strain Nissle 1917-from bench to bedside and back: history of a special *Escherichia coli* strain with probiotic properties. *FEMS Microbiol Lett* **363**, (2016).
24. T. M. Wassenaar, Insights from 100 Years of Research with Probiotic *E. Coli*. *Eur J Microbiol Immunol (Bp)* **6**, 147-161 (2016).
25. P. D. Frenzen, A. Drake, F. J. Angulo, Economic cost of illness due to *Escherichia coli* O157 infections in the United States. *J Food Prot* **68**, 2623-2630 (2005).
26. J. Tilden, Jr. *et al.*, A new route of transmission for *Escherichia coli*: infection from dry fermented salami. *Am J Public Health* **86**, 1142-1145 (1996).
27. Y. Nguyen, V. Sperandio, Enterohemorrhagic *E. coli* (EHEC) pathogenesis. *Front Cell Infect Microbiol* **2**, 90 (2012).
28. J. M. Rangel, P. H. Sparling, C. Crowe, P. M. Griffin, D. L. Swerdlow, Epidemiology of *Escherichia coli* O157:H7 outbreaks, United States, 1982-2002. *Emerg Infect Dis* **11**, 603-609 (2005).
29. E. Kintz, J. Brainard, L. Hooper, P. Hunter, Transmission pathways for sporadic Shiga-toxin producing *E. coli* infections: A systematic review and meta-analysis. *Int J Hyg Environ Health* **220**, 57-67 (2017).
30. B. P. Bell *et al.*, Predictors of hemolytic uremic syndrome in children during a large outbreak of *Escherichia coli* O157:H7 infections. *Pediatrics* **100**, E12 (1997).
31. C. L. Mayer, C. S. Leibowitz, S. Kurosawa, D. J. Stearns-Kurosawa, Shiga toxins and the pathophysiology of hemolytic uremic syndrome in humans and animals. *Toxins (Basel)* **4**, 1261-1287 (2012).
32. S. B. Freedman *et al.*, Shiga Toxin-Producing *Escherichia coli* Infection, Antibiotics, and Risk of Developing Hemolytic Uremic Syndrome: A Meta-analysis. *Clin Infect Dis* **62**, 1251-1258 (2016).
33. M. J. Farfan, L. Cantero, R. Vidal, D. J. Botkin, A. G. Torres, Long polar fimbriae of enterohemorrhagic *Escherichia coli* O157:H7 bind to extracellular matrix proteins. *Infect Immun* **79**, 3744-3750 (2011).
34. B. D. McWilliams, A. G. Torres, EHEC Adhesins. *Microbiol Spectr* **2**, EHEC-0003-2013- (2014).
35. S. L. Slater, A. M. Sagfors, D. J. Pollard, D. Ruano-Gallego, G. Frankel, The Type III Secretion System of Pathogenic *Escherichia coli*. *Curr Top Microbiol Immunol* **416**, 51-72 (2018).
36. Y. Lai, I. Rosenshine, J. M. Leong, G. Frankel, Intimate host attachment: enteropathogenic and enterohaemorrhagic *Escherichia coli*. *Cell Microbiol* **15**, 1796-1808 (2013).
37. T. K. McDaniel, K. G. Jarvis, M. S. Sonnenberg, J. B. Kaper, A genetic locus of enterocyte effacement conserved among diverse enterobacterial pathogens. *Proc Natl Acad Sci U S A* **92**, 1664-1668 (1995).
38. S. J. Elliott *et al.*, The locus of enterocyte effacement (LEE)-encoded regulator controls expression of both LEE- and non-LEE-encoded virulence factors in enteropathogenic and enterohemorrhagic *Escherichia coli*. *Infect Immun* **68**, 6115-6126 (2000).

39. F. M. Franzin, M. P. Sircili, Locus of enterocyte effacement: a pathogenicity island involved in the virulence of enteropathogenic and enterohemorrhagic *Escherichia coli* subjected to a complex network of gene regulation. *Biomed Res Int* **2015**, 534738 (2015).
40. S. Gruenheid *et al.*, Identification and characterization of NleA, a non-LEE-encoded type III translocated virulence factor of enterohaemorrhagic *Escherichia coli* O157:H7. *Mol Microbiol* **51**, 1233-1249 (2004).
41. M. Larzabal, W. Marques Da Silva, N. A. Riviere, A. A. Cataldi, Novel Effector Protein EspY3 of Type III Secretion System from Enterohemorrhagic *Escherichia coli* Is Localized in Actin Pedestals. *Microorganisms* **6**, (2018).
42. T. Tobe *et al.*, An extensive repertoire of type III secretion effectors in *Escherichia coli* O157 and the role of lambdoid phages in their dissemination. *Proc Natl Acad Sci U S A* **103**, 14941-14946 (2006).
43. A. Vossenkämper, T. T. MacDonald, O. Marchès, Always one step ahead: How pathogenic bacteria use the type III secretion system to manipulate the intestinal mucosal immune system. *Journal of Inflammation* **8**, 1-10 (2011).
44. J. M. Ritchie, Animal Models of Enterohemorrhagic *Escherichia coli* Infection. *Microbiol Spectr* **2**, Ehec-0022-2013 (2014).
45. E. A. Wadolkowski, J. A. Burris, A. D. O'Brien, Mouse model for colonization and disease caused by enterohemorrhagic *Escherichia coli* O157:H7. *Infect Immun* **58**, 2438-2445 (1990).
46. M. P. Leatham *et al.*, Precolonized human commensal *Escherichia coli* strains serve as a barrier to *E. coli* O157:H7 growth in the streptomycin-treated mouse intestine. *Infect Immun* **77**, 2876-2886 (2009).
47. W. Deng, Y. Li, B. A. Vallance, B. B. Finlay, in *Infect Immun*. (2001), vol. 69, pp. 6323-6335.
48. W. Deng *et al.*, Dissecting virulence: systematic and functional analyses of a pathogenicity island. *Proc Natl Acad Sci U S A* **101**, 3597-3602 (2004).
49. R. Mundy, T. T. MacDonald, G. Dougan, G. Frankel, S. Wiles, *Citrobacter rodentium* of mice and man. *Cell Microbiol* **7**, 1697-1706 (2005).
50. N. K. Petty *et al.*, The *Citrobacter rodentium* genome sequence reveals convergent evolution with human pathogenic *Escherichia coli*. *J Bacteriol* **192**, 525-538 (2010).
51. J. W. Collins *et al.*, *Citrobacter rodentium*: infection, inflammation and the microbiota. *Nat Rev Microbiol* **12**, 612-623 (2014).
52. N. Bouladoux, O. J. Harrison, Y. Belkaid, The Mouse Model of Infection with *Citrobacter rodentium*. *Curr Protoc Immunol* **119**, 19.15.11-19.15.25 (2017).
53. J. B. Kaper, J. P. Nataro, H. L. T. Mobley, Pathogenic *Escherichia coli*. *Nature Reviews Microbiology* **2**, 123-140 (2004).
54. D. B. Schauer, S. Falkow, Attaching and effacing locus of a *Citrobacter freundii* biotype that causes transmissible murine colonic hyperplasia. *Infect Immun* **61**, 2486-2492 (1993).
55. P. C. Brennan, T. E. Fritz, R. J. Flynn, C. M. Poole, CITROBACTER FREUNDII ASSOCIATED WITH DIARRHEA IN A LABORATORY MICE. *Lab Anim Care* **15**, 266-275 (1965).
56. S. Wiles, K. M. Pickard, K. Peng, T. T. MacDonald, G. Frankel, in *Infect Immun*. (2006), vol. 74, pp. 5391-5396.
57. N. Kamada *et al.*, Regulated Virulence Controls the Ability of a Pathogen to Compete with the Gut Microbiota. *Science* **336**, 1325-1329 (2012).

58. K. Y. Ebino, Studies on coprophagy in experimental animals. *Jikken Dobutsu* **42**, 1-9 (1993).
59. S. Wiles, G. Dougan, G. Frankel, Emergence of a 'hyperinfectious' bacterial state after passage of *Citrobacter rodentium* through the host gastrointestinal tract. *Cell Microbiol* **7**, 1163-1172 (2005).
60. A. L. Bishop, S. Wiles, G. Dougan, G. Frankel, Cell attachment properties and infectivity of host-adapted and environmentally adapted *Citrobacter rodentium*. *Microbes Infect* **9**, 1316-1324 (2007).
61. C. L. Randle, P. W. Albro, J. C. Dittmer, The phosphoglyceride composition of Gram-negative bacteria and the changes in composition during growth. *Biochim Biophys Acta* **187**, 214-220 (1969).
62. P. B. Cotton, Non-dietary lipid in the intestinal lumen. *Gut* **13**, 675-681 (1972).
63. O. Tsoy, D. Ravcheev, A. Mushegian, Comparative genomics of ethanolamine utilization. *J Bacteriol* **191**, 7157-7164 (2009).
64. S. Krysenko *et al.*, Initial Metabolic Step of a Novel Ethanolamine Utilization Pathway and Its Regulation in *Streptomyces coelicolor* M145. *mBio* **10**, (2019).
65. B. S. Francisco, X. Zhang, K. Whalen, J. Gerlt, A Novel Pathway for Bacterial Ethanolamine Metabolism. (2015).
66. B. M. Babior, T. H. Moss, D. C. Gould, The Mechanism of Action of Ethanolamine Ammonia Lyase, a B<sub>12</sub>-dependent Enzyme. (1972).
67. D. M. Roof, J. R. Roth, Ethanolamine utilization in *Salmonella typhimurium*. *J Bacteriol* **170**, 3855-3863 (1988).
68. D. A. Garsin, Ethanolamine utilization in bacterial pathogens: roles and regulation. *Nat Rev Microbiol* **8**, 290-295 (2010).
69. K. Mori, R. Bando, N. Hieda, T. Toraya, Identification of a reactivating factor for adenosylcobalamin-dependent ethanolamine ammonia lyase. *J Bacteriol* **186**, 6845-6854 (2004).
70. E. Kofoed, C. Rappleye, I. Stojiljkovic, J. Roth, The 17-gene ethanolamine (eut) operon of *Salmonella typhimurium* encodes five homologues of carboxysome shell proteins. *J Bacteriol* **181**, 5317-5329 (1999).
71. S. R. Brinsmade, T. Paldon, J. C. Escalante-Semerena, Minimal functions and physiological conditions required for growth of *salmonella enterica* on ethanolamine in the absence of the metabolosome. *J Bacteriol* **187**, 8039-8046 (2005).
72. N. R. Buan, S.-J. Suh, J. C. Escalante-Semerena, The eutT Gene of *Salmonella enterica* Encodes an Oxygen-Labile, Metal-Containing ATP:Corrinoid Adenosyltransferase Enzyme. (2004).
73. C. J. Anderson, J. Satkovich, V. K. Koseoglu, H. Agaisse, M. M. Kendall, The Ethanolamine Permease EutH Promotes Vacuole Adaptation of *Salmonella enterica* and *Listeria monocytogenes* during Macrophage Infection. *Infect Immun* **86**, (2018).
74. I. Stojiljkovic, A. J. Baumler, F. Heffron, Ethanolamine utilization in *Salmonella typhimurium*: nucleotide sequence, protein expression, and mutational analysis of the cchA cchB eutE eutJ eutG eutH gene cluster. *J Bacteriol* **177**, 1357-1366 (1995).
75. J. T. Penrod, J. R. Roth, Conserving a volatile metabolite: a role for carboxysome-like organelles in *Salmonella enterica*. *J Bacteriol* **188**, 2865-2874 (2006).

76. D. M. Roof, J. R. Roth, Functions required for vitamin B12-dependent ethanolamine utilization in *Salmonella typhimurium*. *J Bacteriol* **171**, 3316-3323 (1989).
77. S. R. Brinsmade, J. C. Escalante-Semerena, The *eutD* gene of *Salmonella enterica* encodes a protein with phosphotransacetylase enzyme activity. *J Bacteriol* **186**, 1890-1892 (2004).
78. V. J. Starai, J. Garrity, J. C. Escalante-Semerena, Acetate excretion during growth of *Salmonella enterica* on ethanolamine requires phosphotransacetylase (*EutD*) activity, and acetate recapture requires acetyl-CoA synthetase (*Acs*) and phosphotransacetylase (*Pta*) activities. *Microbiology* **151**, 3793-3801 (2005).
79. D. M. Roof, J. R. Roth, Autogenous regulation of ethanolamine utilization by a transcriptional activator of the *eut* operon in *Salmonella typhimurium*. *J Bacteriol* **174**, 6634-6643 (1992).
80. M. T. Gallegos, R. Schleif, A. Bairoch, K. Hofmann, J. L. Ramos, Arac/XylS family of transcriptional regulators. *Microbiol Mol Biol Rev* **61**, 393-410 (1997).
81. D. H. Luzader, D. E. Clark, L. A. Gonyar, M. M. Kendall, *EutR* is a direct regulator of genes that contribute to metabolism and virulence in enterohemorrhagic *Escherichia coli* O157:H7. *J Bacteriol* **195**, 4947-4953 (2013).
82. J. R. Mellin *et al.*, Riboswitches. Sequestration of a two-component response regulator by a riboswitch-regulated noncoding RNA. *Science* **345**, 940-943 (2014).
83. S. DebRoy *et al.*, Riboswitches. A riboswitch-containing sRNA controls gene expression by sequestration of a response regulator. *Science* **345**, 937-940 (2014).
84. Y. Bertin *et al.*, Enterohaemorrhagic *Escherichia coli* gains a competitive advantage by using ethanolamine as a nitrogen source in the bovine intestinal content. *Environ Microbiol* **13**, 365-377 (2011).
85. A. Maadani, K. A. Fox, E. Mylonakis, D. A. Garsin, *Enterococcus faecalis* mutations affecting virulence in the *Caenorhabditis elegans* model host. *Infect Immun* **75**, 2634-2637 (2007).
86. C. J. Anderson, D. E. Clark, M. Adli, M. M. Kendall, Ethanolamine Signaling Promotes *Salmonella* Niche Recognition and Adaptation during Infection. *PLoS Pathog* **11**, e1005278 (2015).
87. P. Thiennimitr *et al.*, Intestinal inflammation allows *Salmonella* to use ethanolamine to compete with the microbiota. *Proc Natl Acad Sci U S A* **108**, 17480-17485 (2011).
88. M. M. Kendall, C. C. Gruber, C. T. Parker, V. Sperandio, Ethanolamine controls expression of genes encoding components involved in interkingdom signaling and virulence in enterohemorrhagic *Escherichia coli* O157:H7. *MBio* **3**, (2012).
89. A. Sintsova, S. Smith, S. Subashchandrabose, H. L. Mobley, Role of Ethanolamine Utilization Genes in Host Colonization during Urinary Tract Infection. *Infect Immun* **86**, (2018).
90. K. L. Nawrocki, D. Wetzel, J. B. Jones, E. C. Woods, S. M. McBride, Ethanolamine is a valuable nutrient source that impacts *Clostridium difficile* pathogenesis. *Environ Microbiol* **20**, 1419-1435 (2018).
91. L. A. Gonyar, M. M. Kendall, Ethanolamine and choline promote expression of putative and characterized fimbriae in enterohemorrhagic *Escherichia coli* O157:H7. *Infect Immun* **82**, 193-201 (2014).

92. B. R. Lundgren *et al.*, Ethanolamine Catabolism in *Pseudomonas aeruginosa* PAO1 Is Regulated by the Enhancer-Binding Protein EatR (PA4021) and the Alternative Sigma Factor RpoN. (2016).
93. M. de Graaf *et al.*, Sustained fecal-oral human-to-human transmission following a zoonotic event. *Curr Opin Virol* **22**, 1-6 (2017).
94. E. Scallan *et al.*, Foodborne illness acquired in the United States--major pathogens. *Emerg Infect Dis* **17**, 7-15 (2011).
95. S. Almagro-Moreno, R. K. Taylor, Cholera: Environmental Reservoirs and Impact on Disease Transmission. *Microbiol Spectr* **1**, (2013).
96. J. N. Eisenberg, J. Trostle, R. J. Sorensen, K. F. Shields, Toward a Systems Approach to Enteric Pathogen Transmission: From Individual Independence to Community Interdependence. *Annu Rev Public Health* **33**, 239-257 (2012).
97. E. S. McKenney, M. M. Kendall, Microbiota and pathogen 'pas de deux': setting up and breaking down barriers to intestinal infection. *Pathog Dis* **74**, (2016).
98. K. G. Kaval, D. A. Garsin, Ethanolamine Utilization in Bacteria. *MBio* **9**, (2018).
99. K. G. Kaval *et al.*, Loss of Ethanolamine Utilization in *Enterococcus faecalis* Increases Gastrointestinal Tract Colonization. *mBio* **9**, (2018).
100. A. Segura, P. Auffret, C. Klopp, Y. Bertin, E. Forano, in *Stand Genomic Sci.* (England, 2017), vol. 12, pp. 61.
101. T. Conway, P. S. Cohen, Commensal and Pathogenic *Escherichia coli* Metabolism in the Gut. *Microbiol Spectr* **3**, (2015).
102. F. R, in *Fuller R (ed), Probiotics. The scientific basis.* (Chapman and Hall, London, United Kingdom, 1992), pp. 355 – 376.
103. C. M. Blackwell, F. A. Scarlett, J. M. Turner, Microbial metabolism of amino alcohols. Control of formation and stability of partially purified ethanolamine ammonia-lyase in *Escherichia coli*. *J Gen Microbiol* **98**, 133-139 (1977).
104. D. A. Garsin, Ethanolamine: a signal to commence a host-associated lifestyle? *mBio* **3**, e00172-00112 (2012).
105. D. Barnett Foster, Modulation of the enterohemorrhagic *E. coli* virulence program through the human gastrointestinal tract. *Virulence* **4**, 315-323 (2013).
106. J. O. Korbel *et al.*, Systematic association of genes to phenotypes by genome and literature mining. *PLoS Biol* **3**, e134 (2005).
107. L. Staib, T. M. Fuchs, From food to cell: nutrient exploitation strategies of enteropathogens. *Microbiology* **160**, 1020-1039 (2014).
108. K. Dadswell *et al.*, in *Infect Immun.* (2019), vol. 87.
109. J. Sambrook, E. F. Fritsch, T. Maniatis. (Cold Spring Harbor Laboratory Press, Cold Spring Harbor, NY, 1989).
110. T. Brooks, C. W. Keevil, A simple artificial urine for the growth of urinary pathogens. *Lett Appl Microbiol* **24**, 203-206 (1997).
111. I. Piazza *et al.*, A Map of Protein-Metabolite Interactions Reveals Principles of Chemical Communication. *Cell* **172**, 358-372.e323 (2018).
112. K. A. Datsenko, B. L. Wanner, One-step inactivation of chromosomal genes in *Escherichia coli* K-12 using PCR products. *Proc Natl Acad Sci U S A* **97**, 6640-6645 (2000).
113. M. C. Lane, C. J. Alteri, S. N. Smith, H. L. Mobley, Expression of flagella is coincident with uropathogenic *Escherichia coli* ascension to the upper urinary tract. *Proc Natl Acad Sci U S A* **104**, 16669-16674 (2007).

114. M. M. Kendall, D. A. Rasko, V. Sperandio, The LysR-type regulator QseA regulates both characterized and putative virulence genes in enterohaemorrhagic *Escherichia coli* O157:H7. *Mol Microbiol* **76**, 1306-1321 (2010).
115. L. K.J. (PE Applied Biosystems, 1997), vol. User Bulletin no 2, pp. 777802-778002.
116. W. A. Ferens, C. J. Hovde, *Escherichia coli* O157:H7: animal reservoir and sources of human infection. *Foodborne Pathog Dis* **8**, 465-487 (2011).
117. K. E. Heiman, R. K. Mody, S. D. Johnson, P. M. Griffin, L. H. Gould, in *Emerg Infect Dis.* (2015), vol. 21, pp. 1293-1301.
118. A. Kanayama *et al.*, Enterohemorrhagic *Escherichia coli* outbreaks related to childcare facilities in Japan, 2010-2013. *BMC Infect Dis* **15**, 539 (2015).
119. C. H. Pai *et al.*, Epidemiology of sporadic diarrhea due to verocytotoxin-producing *Escherichia coli*: a two-year prospective study. *J Infect Dis* **157**, 1054-1057 (1988).
120. M. Ota, T. Kamigaki, S. Mimura, K. Nakashima, T. Ogami, An enterohaemorrhagic *Escherichia coli* outbreak spread through the environment at an institute for people with intellectual disabilities in Japan in 2005. *Western Pac Surveill Response J* **10**, 14-21 (2019).
121. C. M. Blackwell, F. A. Scarlett, J. M. Turner, Ethanolamine catabolism by bacteria, including *Escherichia coli*. *Biochem Soc Trans* **4**, 495-497 (1976).
122. C. M. Blackwell, J. M. Turner, Microbial metabolism of amino alcohols. Purification and properties of coenzyme B12-dependent ethanolamine ammonia-lyase of *Escherichia coli*. *Biochem J* **175**, 555-563 (1978).
123. M. E. Wickham, N. F. Brown, E. C. Boyle, B. K. Coombes, B. B. Finlay, Virulence is positively selected by transmission success between mammalian hosts. *Curr Biol* **17**, 783-788 (2007).
124. C. Mullineaux-Sanders *et al.*, *Citrobacter rodentium* –host–microbiota interactions: immunity, bioenergetics and metabolism. *Nature Reviews Microbiology* **17**, 701-715 (2019).
125. V. A. García-Angulo, W. Deng, N. A. Thomas, B. B. Finlay, J. L. Puente, in *J Bacteriol.* (2008), vol. 190, pp. 2388-2399.
126. E. Hart *et al.*, RegA, an AraC-like protein, is a global transcriptional regulator that controls virulence gene expression in *Citrobacter rodentium*. *Infect Immun* **76**, 5247-5256 (2008).
127. M. Simovitch *et al.*, EspM inhibits pedestal formation by enterohaemorrhagic *Escherichia coli* and enteropathogenic *E. coli* and disrupts the architecture of a polarized epithelial monolayer. *Cell Microbiol* **12**, 489-505 (2010).
128. W. Deng, B. A. Vallance, Y. Li, J. L. Puente, B. B. Finlay, *Citrobacter rodentium* translocated intimin receptor (Tir) is an essential virulence factor needed for actin condensation, intestinal colonization and colonic hyperplasia in mice. *Mol Microbiol* **48**, 95-115 (2003).
129. R. M. Russell, F. C. Sharp, D. A. Rasko, V. Sperandio, QseA and GrIR/GrIA regulation of the locus of enterocyte effacement genes in enterohemorrhagic *Escherichia coli*. *J Bacteriol* **189**, 5387-5392 (2007).
130. S. Wiles *et al.*, Organ specificity, colonization and clearance dynamics in vivo following oral challenges with the murine pathogen *Citrobacter rodentium*. *Cell Microbiol* **6**, 963-972 (2004).

131. M. J. Ormsby *et al.*, Inflammation associated ethanolamine facilitates infection by Crohn's disease-linked adherent-invasive Escherichia coli. *EBioMedicine* **43**, 325-332 (2019).
132. J. P. R. Connolly *et al.*, Host-associated niche metabolism controls enteric infection through fine-tuning the regulation of type 3 secretion. *Nat Commun* **9**, 4187 (2018).
133. A. A. Crofts *et al.*, Enterotoxigenic E. coli virulence gene regulation in human infections. *Proc Natl Acad Sci U S A* **115**, E8968-e8976 (2018).
134. S. Buschor *et al.*, in *PLoS Pathog.* (2017), vol. 13.
135. N. Kamada *et al.*, Humoral Immunity in the Gut Selectively Targets Phenotypically Virulent Attaching-and-Effacing Bacteria for Intraluminal Elimination. *Cell Host Microbe* **17**, 617-627 (2015).
136. P. A. Cotter, V. J. DiRita, Bacterial virulence gene regulation: an evolutionary perspective. *Annu Rev Microbiol* **54**, 519-565 (2000).
137. S. Kitamoto, H. Nagao-Kitamoto, P. Kuffa, N. Kamada, Regulation of virulence: the rise and fall of gastrointestinal pathogens. *J Gastroenterol* **51**, 195-205 (2016).
138. R. Mundy *et al.*, Identification of a novel type IV pilus gene cluster required for gastrointestinal colonization of Citrobacter rodentium. *Mol Microbiol* **48**, 795-809 (2003).
139. S. Alizon, A. Hurford, N. Mideo, M. Van Baalen, Virulence evolution and the trade-off hypothesis: history, current state of affairs and the future. *J Evol Biol* **22**, 245-259 (2009).
140. C. J. Anderson, D. E. Clark, M. Adli, M. M. Kendall, Ethanolamine signaling promotes *Salmonella* niche recognition and adaptation during infection. *PLoS Pathog.* **11**, e1005278 (2015).
141. A. Sittka *et al.*, Deep sequencing analysis of small noncoding RNA and mRNA targets of the global post-transcriptional regulator, Hfq. *PLoS Genet* **4**, e1000163 (2008).
142. I. Ambite *et al.*, Molecular Basis of Acute Cystitis Reveals Susceptibility Genes and Immunotherapeutic Targets. *PLoS Pathog* **12**, e1005848 (2016).
143. A. Waldhuber *et al.*, Uropathogenic Escherichia coli strain CFT073 disrupts NLRP3 inflammasome activation. *J Clin Invest* **126**, 2425-2436 (2016).
144. F. Girard, V. F. Crepin, G. Frankel, Modelling of Infection by Enteropathogenic Escherichia coli Strains in Lineages 2 and 4 Ex Vivo and In Vivo by Using Citrobacter rodentium Expressing TccP. (2009).
145. A. Bishop, S. Wiles, G. Dougan, G. Frankel, Cell attachment properties and infectivity of host-adapted and environmentally adapted Citrobacter rodentium. - PubMed - NCBI. *Microbes Infect.*, (2019).
146. Z. Mukandavire *et al.*, Estimating the reproductive numbers for the 2008–2009 cholera outbreaks in Zimbabwe. (2011).
147. S. M. Butler *et al.*, Cholera stool bacteria repress chemotaxis to increase infectivity. *Mol Microbiol* **60**, 417-426 (2006).
148. N. T. Perna *et al.*, Genome sequence of enterohaemorrhagic Escherichia coli O157:H7. *Nature* **409**, 529-533 (2001).
149. F. Madeira, Park, YM., Lee, J., Buso, N., Gur, T., Madhusoodanan, N., Basutkar, P., Tivey, ARN., Potter, SC., Finn, RD. and Lopez, R., The EMBL-EBI search and sequence analysis tools APIs in 2019. *Nucleic Acids Res* **47(W1)**, W636–W641 (2019).

150. E. M. Melson, M. M. Kendall, The sRNA DicF integrates oxygen sensing to enhance enterohemorrhagic *Escherichia coli* virulence via distinctive RNA control mechanisms. *Proc Natl Acad Sci U S A* **116**, 14210-14215 (2019).
151. K. J. Livak, ABI Prism 7700 Sequence Detection System. *User Bulletin no. 2, PE Applied Biosystems* **4303859B**, 777802-778002 (1997).
152. V. A. Rhodius, J. T. Wade, Technical considerations in using DNA microarrays to define regulons. *Methods* **47**, 63-73 (2009).
153. N. A. Pchelinstev, P. D. Adams, D. M. Nelson, Critical Parameters for Efficient Sonication and Improved Chromatin Immunoprecipitation of High Molecular Weight Proteins. *PLoS ONE* **11**, e0148023 (2016).
154. A. E. Santiago *et al.*, The AraC Negative Regulator family modulates the activity of histone-like proteins in pathogenic bacteria. *PLoS Pathog* **13**, e1006545 (2017).
155. C. A. Lopez *et al.*, Virulence factors enhance *Citrobacter rodentium* expansion through aerobic respiration. *Science* **353**, 1249-1253 (2016).
156. C. Bradbeer, The clostridial fermentations of choline and ethanolamine. 1. Preparation and properties of cell-free extracts. *J Biol Chem* **240**, 4669-4674 (1965).
157. C. Bradbeer, The clostridial fermentations of choline and ethanolamine. II. Requirement for a cobamide coenzyme by an ethanolamine deaminase. *J Biol Chem* **240**, 4675-4681 (1965).
158. P. M. Griffin *et al.*, Illnesses associated with *Escherichia coli* O157:H7 infections. A broad clinical spectrum. *Ann Intern Med* **109**, 705-712 (1988).